



Destroy this report when no longer needed. Do not return  
it to the originator.

The findings in this report are not to be construed as an official  
Department of the Army position unless so designated  
by other authorized documents.

The contents of this report are not to be used for  
advertising, publication, or promotional purposes.  
Citation of trade names does not constitute an  
*official endorsement or approval of the use of*  
such commercial products.



13. (Concluded).

Based on these limited case studies, recommendations on modeling techniques for various conditions are provided. Appendixes are included to describe various unique characteristics included in the structural analysis program.

PREFACE

This report is the first of a series which will describe the research conducted as part of a Computer-Aided Structural Engineering (CASE) Project effort entitled "Computer-Aided, Field-Verified Structural Evaluation." The CASE Project is managed by the Scientific and Engineering Applications Center (S&EAC) of the Computer-Aided Engineering Division (CAED), Information Technology Laboratory (ITL), US Army Engineer Waterways Experiment Station (WES). The CASE Project is funded by the Civil Works Directorate of Headquarters, US Army Corps of Engineers (HQUSACE). Mr. Cameron Chasten monitored this work under the general supervision of Mr. H. Wayne Jones, Chief, S&EAC, and Dr. N. Radhakrishnan, Director, ITL.

The work was performed by Bridge Diagnostics Incorporated under USACE contract DACW39-91-C-0102. Principal Investigators were Mr. Brett Commander, Mr. Jeff Schulz, and Dr. George Goble.

At the time of publication of this report, Director of WES was Dr. Robert W. Whalin. Commander was COL Leonard G. Hassell, EN.

DTIC QUALITY INSPECTED 3

Accession For	
NTIS <del>SEARCH</del>	<input checked="" type="checkbox"/>
DWIO TAB	<input type="checkbox"/>
Unannounced	<input type="checkbox"/>
Justification	
Ev.	
Distribution/	
Availability Codes	
Avail and/or	
Dist	Special
A-1	

## CONTENTS

	<u>Page</u>
PREFACE . . . . .	1
CONVERSION FACTORS, NON-SI TO SI (METRIC) UNITS OF MEASUREMENT . . . . .	4
PART I: INTRODUCTION . . . . .	5
PART II: NUMERICAL REPRESENTATION OF MITER GATES . . . . .	7
Objectives . . . . .	7
Selection of Analysis Software . . . . .	7
Analysis Capabilities and Limitations . . . . .	8
Representation of Miter Gates . . . . .	11
PART III: CASE STUDIES . . . . .	21
Lock Gate 26, Mississippi River . . . . .	21
John Hollis Bankhead Lock and Dam . . . . .	28
PART IV: GENERAL CONCLUSIONS . . . . .	33
Vertically Framed Miter Gates . . . . .	33
Horizontally Framed Miter Gates . . . . .	33
PART V: FUTURE IMPLEMENTATIONS . . . . .	35
REFERENCES . . . . .	37
APPENDIX A: PARAMETER OPTIMIZATION . . . . .	A1
APPENDIX B: COMPUTER IMPLEMENTATION . . . . .	B1
APPENDIX C: ANALYSIS INPUT AND RESULT DATA . . . . .	C1
APPENDIX D: A DEVELOPMENT OF WARPING TORSION TERMS . . . . .	D1

LIST OF TABLES

<u>No.</u>		<u>Page</u>
1	Strains at Top Girder (Center Cross Section) . . . . .	26
2	Axial Force and Flexural Moment, Top Girder Center . . . . .	26
3	Axial Force and Flexural Moment, Top Girder Miter End . . . . .	27
4	Axial Force and Flexural Moment, Top Girder Quoin End . . . . .	27

LIST OF FIGURES

<u>No.</u>		<u>Page</u>
1	Representation of a vertically framed miter gate . . . . .	15
2	Simple grid model of a horizontally framed miter gate . . . . .	16
3	Refined grid model for a horizontally framed miter gate . . . . .	18
4	3-D representation of two horizontal girders . . . . .	20
5	Representation of roller supports to model symmetry . . . . .	24
6	Transducer locations on top girder . . . . .	25
7	(A) Degrees of freedom associated with plate-membrane element (B) Modeling deficiency due to missing rotational stiffness terms . . . . .	31
8	Mesh refinement approach to modeling in-plane bending . . . . .	31
9	Frame element with built-in eccentricity term . . . . .	36
D1	Restrained warping torsion in beam flanges . . . . .	D2

CONVERSION FACTORS, NON-SI TO SI (METRIC)  
UNITS OF MEASUREMENT

Non-SI units of measurement used in this report can be converted to SI (metric) units as follows:

<u>Multiply</u>	<u>By</u>	<u>To Obtain</u>
feet	0.3048	meters
inches	0.0254	meters
kip-foot	1355.818	newton-meter
kips per square inch (ksi)	6894.757	kilopascals

COMPUTER-AIDED, FIELD-VERIFIED  
STRUCTURAL EVALUATION

DEVELOPMENT OF COMPUTER MODELING TECHNIQUES  
FOR MITER LOCK GATES

PART I: INTRODUCTION

1. There are over 160 commercially active locks (including over 200 lock chambers) on the United States inland and intracoastal waterway systems. The ages of these lock chambers range from one year to over 150 years. Approximately 40 percent of the locks are over 50 years old and the median age of all chambers is approximately 35 years (USACE 1988). Most of the locks include miter lock gates which are either horizontally framed or vertically framed. Due to the deterioration with age and the large number of miter gates which are in operation, structural evaluation is necessary to assess existing strength and safety of many of these lock gates. The primary goal of the project reported herein is to develop an evaluation system incorporating analytical and experimental techniques which may be used to assess the strength and safety of miter lock gates.

2. Through the combined use of modern computer software, digital data acquisition technology, and experimental testing, a simple realistic approach to determine the structural behavior of miter lock gates is possible. Rather than basing a structural evaluation solely on analytical techniques or experimental measurements, the proposed method integrates the two. Sophisticated finite element analytical models can be developed to predict the behavior of any structure. However, for any analysis many assumptions must be used in the representation of structural geometry and material properties, and it is not possible to exactly represent the behavior of complex structures. Additionally, sophisticated experimental techniques are available to measure a structure's response to various loadings, but for a given experiment only a few selected points on a structure can be monitored. By combining analytical and experimental techniques an optimum system which incorporates the benefits of both techniques can be developed. Analytical and experimental results can be compared, and the analytical model can be systematically modified until it reproduces the behavior observed under experimental conditions.

3. Such an integrated system has been developed and successfully implemented for highway bridges by the University of Colorado. This work was accomplished during the completion of two research projects sponsored by the Pennsylvania Department of Transportation (PennDOT) and the Federal Highway Administration (FHWA) (Goble, Schulz, and Commander 1990a and Goble et al. 1991). A principal goal of these studies was to develop a systematic approach to evaluating ambiguous structural parameters so as to improve the accuracy of analytical models. The quality of the models was evaluated by comparing theoretical structural responses with experimental (field) strain measurements.

4. For the current study, the modeling and analysis procedures that were used for highway bridges have been modified for use in the evaluation of vertically and horizontally framed miter gates. This report describes the methods used to represent miter gates analytically, the structural analysis capabilities of the software, and the results of two case studies performed on miter gates for which field data had been acquired.

## PART II: NUMERICAL REPRESENTATION OF MITER GATES

### Objectives

5. One of the primary goals in the initial phase of this project is to develop the analytical modeling procedures required to represent the structural responses of miter gates subjected to normal service loads. The modeling procedure should be sufficiently detailed to simulate the indeterminate load transfer characteristics of miter gates yet be efficient and straightforward enough to be used on a routine basis.

6. In addition to providing modeling and analysis procedures, an approach for making modifications to the analytical model until its load response is similar to that of the actual structure is required. Quite often, the numerical representation of an actual structure is developed using a considerable amount of subjective judgment. For example, the structural geometry might be simplified or a material or structural property might not be well defined, particularly when representing a complex component or a damaged element. It is desirable to quantify these obscure properties such that a numerical model can provide load responses similar to those of the real structure. This requires a method of comparing measured responses with analytical results and systematically modifying the modeling parameters until the two correlate. With this type of iterative process, the final analytical model provides a relatively accurate representation of the actual lock gate. The response of a structure under various load conditions can then be simulated using the analytical computer model, and predictions for response can be made for any location on the structure. With this approach, the overall structural performance can be evaluated based on the correlation with experimental results obtained from a few locations.

### Selection of Analysis Software

7. Miter gates are complex indeterminate structures, therefore, a finite element approach is the most logical choice for an analysis method. Finite element procedures are relatively well understood and widely used in analysis today.

8. Due to the unique nature of the project goals, commercial software packages that fulfill the requirements for both modeling and iterative

parameter modification do not exist. However, software has been developed at the University of Colorado to address these objectives (Goble, Schulz, and Commander 1990a and Goble et al. 1991). The computer program developed at the University of Colorado, Structural Analysis and Correlation (SAC), meets most of the requirements of this project since it has advanced modeling capabilities and includes a parameter optimization algorithm. To account for geometry and loading characteristics, various features were added to customize the program for miter gate modeling and analysis.

### Analysis Capabilities and Limitations

#### Structural geometry and element library

9. Although it is desirable to maintain as much simplicity as possible in the modeling of lock gates, SAC includes three-dimensional modeling capability. Nodal displacements are represented with translations in three orthogonal directions and rotations about three orthogonal axes (six degrees of freedom per node). The overall structural geometry is defined within a single global Cartesian coordinate system, and a local coordinate system is included for each individual element. Thus, strains and internal forces can be represented with respect to element orientations and there are no limitations to the orientation of a member within a structure.

10. In the current version of SAC, structures can be represented with the following three basic modeling components:

- a. Frame elements. Girders, beams, and diagonal members are simulated with space frame elements. These elements are one-dimensional in geometry since they are defined by two nodes; however, they have stiffness properties to resist loads and displacements in three dimensions.
- b. Plate-membrane elements. Skin plates, and for refined modeling, girder webs and flanges can be modeled with the use of rectangular membrane-plate elements. The membrane-plate element is a hybrid of two separate quadrilateral elements: a rectangular plate bending element and a four-node membrane element. The plate bending element is capable of modeling an out-of-plane displacement and rotations about two in-plane axes. The membrane degrees of freedom consist of translations along the two in-plane axes. Because of the small displacement assumption, the deflections are uncoupled.
- c. Spring elements. Spring elements which may be used to represent elastic supports or semirigid connections are also available. These elements have no spacial dimensions and are defined by translational and/or rotational elastic stiffness constants.

### Load applications

11. The version of SAC developed for bridge studies was modified to include capabilities to model the primary loading characteristics relevant to miter gates. A strong effort has been made to minimize input requirements when implementing common load combinations. The loading applications currently available include:

- a. Dead load. The effect of gravity can easily be applied to a structural model. The material weight of each element group is specified within a material group input data block, and the dead load is simulated by specifying the direction of gravity. The self weight of each structural element is automatically computed and added to the load vector.
- b. Water loading. Water pressure loads are simulated in the models by specifying the water elevation at the upstream and downstream sides of the gate, the direction in which depth is measured, and the unit weight of water. A constant pressure may also be applied. Pressure forces are automatically computed for all plate elements and are represented by equivalent nodal forces which act normal to the element plane. The magnitude of the pressure is based on the average depth of the loaded element.
- c. Nodal loads. Concentrated forces and/or moments can be applied at all nodal locations.
- d. Beam loads. Distributed and/or concentrated loads can be applied to specified frame elements.

Loading capabilities that are likely candidates for future implementation include temperature and prestressing effects.

### Analysis results

12. Equally important to load modeling capabilities is the presentation of analysis results. The number of response types and the clarity of the presentation are vital to the evaluation process. SAC provides a complete listing of analysis results in an easy to read, page style format. There are print options for each response type, so only the output desired will be presented. The following response types are presented in an output data file with ASCII format:

- a. Input echo. To verify data input, the geometry, material information, boundary conditions, and load data are presented in a readable format.
- b. Nodal displacements. As with most finite element programs, the displacements and rotations are tabulated for each node.
- c. Element end forces. Member end forces are computed for all degrees of freedom at each element node for both frame and plate elements. End forces are presented in relation to the local coordinate system of each individual element.

- d. Strains. Strain can be computed at any designated location on specified beam and/or plate elements. These locations usually correspond to the gage locations used during field testing. Strains for frame elements resulting from axial force  $P$  and flexural force about the major axis ( $y$ -axis)  $M_y$  of the element are determined by

$$\epsilon = \frac{\sigma}{E} = \frac{M_y y}{EI_y} + \frac{P}{EA} \quad (1)$$

where  $\sigma$  is the stress,  $E$  the modulus of elasticity,  $y$  the distance to the neutral axis,  $I_y$  the moment of inertia about the  $y$  axis, and  $A$  the cross sectional area.

- e. Support reactions. Reaction forces are computed in global coordinates for each node containing fixed degrees of freedom.
- f. Summation of applied loads. The summation of applied loads is listed for all six degrees of freedom as  $F_x$ ,  $F_y$ ,  $F_z$ ,  $M_x$ ,  $M_y$ , and  $M_z$ , where  $F_i$  is the resultant force in the global  $i$  direction and  $M_i$  is the resultant moment about the global  $i$  axis. These results can be used primarily as a check for the load input data.
- g. Summation of applied loads and reactions. Modeling errors and typographical errors in the input file will lead to erroneous predictions such as for structural instability. The summation of the applied loads and the reactions provides a check to ensure that the sum of forces is zero.
- h. Absolute and percent error. When test data are available, it is often of interest to obtain a comparison of results between the theoretical and measured strains. The differences in the strain results are presented as a summation of the absolute errors at each gage position (total strain difference) and as a percentage error.

#### Limitations of analysis

13. The main limitations to the current version of SAC are that it can only perform static analysis and that all responses are assumed to be linear and elastic. Static analysis is appropriate for normal conditions since the frequency of the applied loads, such as hydraulic loads due to lock filling or impact loads, will generally be much lower than the natural frequency response of miter lock gates. This is particularly true when the gates are in the miter position, since this creates a stiff structural system and thus has a high natural frequency. The requirement of linear and elastic analysis is not a critical limitation since most load applications are normal service loads.

#### Data comparison and parameter evaluation

14. The feature which makes SAC unique from other structural analysis programs is the systematic procedure of comparing the analytical results with

measured responses and evaluating parameters based on these comparisons. SAC includes an optimization procedure which is used to minimize the absolute difference between experimentally obtained and theoretical responses. Individual structural parameters such as torsional stiffness of frame elements or flexural stiffness of damaged sections that are considered to be unknown can be optimized within user defined limits so that the best correlation is obtained. The optimized values can then be incorporated into the model used to evaluate the entire structure. The ability of the optimization procedure to reduce the response error is dependent primarily on the accuracy of the geometry and assumed boundary conditions of the original model. If the original model is basically correct, the error can be minimized and the parameters can be reasonably evaluated. However, if the basic structural characteristics are not well represented, a good correlation between field and numerical results will not be obtained. Hence, the optimization process acts as an indicator of the model quality. A more detailed description of the optimization procedure and algorithm is presented in Appendix A.

#### Representation of Miter Gates

15. In the development of a modeling procedure, it was desired to maintain sufficient simplicity such that the analysis program can effectively be used on a routine basis and can be run on a personal computer (PC). Although there are limitations, modern PC hardware and software are extremely powerful and can be used to perform relatively detailed analysis procedures. (The SAC program has been developed to minimize memory requirements and maximize performance as described in Appendix B.) Therefore, the primary concern is to provide a method which is easily used on a routine basis. It was desired to develop a process for which the complexity involved and time required to generate a finite element model and the associated input data are minimal. Additionally, the process must be such that the analysis will predict accurate results. Simplicity of a model can be viewed in terms of the structural geometry or in terms of the theoretical assumptions and calculations required to compute cross-section properties. There is a direct compromise between geometry and detail. The simpler the geometry, the more complex the individual components (increased complexity in computation of member properties) must be if the same degree of accuracy is to be maintained.

16. Based on several case studies performed by the authors and using studies of a previous CASE project (Emkin, Will, and Goodno 1987) as an example, several models of various geometry configurations were selected for vertically and horizontally framed miter gates. The different models vary in complexity, each having unique advantages and limitations which are discussed below. The model type used in a particular case is dependent on the complexity of the actual structure and the information sought from the analysis. All of the models outlined below can be implemented using SAC. One assumption applied to all of the models is that symmetry is assumed when the gates are in the miter position. Thus, only one gate leaf is modeled and roller supports are applied to the miter end of the leaf to represent the boundary condition imposed by the other leaf. The application of roller supports is discussed in further detail in Part III, "Model details."

#### Vertically framed miter gate

17. Considering load transfer, vertically framed miter gates are relatively simple compared to horizontally framed miter gates. For a mitered vertically framed gate, there are only a few contact points that resist water and impact loads. There is generally only one contact point at the miter end of the leaf near the top girder, two contact points at the quoin end, and a bottom sill supporting the bottom girder. Horizontal loads applied to the vertical members are transferred directly to the top girder and the bottom sill. A vertically framed structure can be represented using a grid model in which all of the vertical girders and beams are simulated by frame elements and are located in a single plane (grid plane). In this approach plate-membrane elements which are used to simulate the skin plate or buckle plates are located in the plane with the vertical members. These elements serve to resist horizontal water loads as well as transfer in-plane loads. The top girder and diagonal members are offset from the grid plane with rigid links, providing a realistic effect of member eccentricity. The horizontal distances (perpendicular to the grid plane) between the structural members and the work line\* closely match the neutral axis location of the members. Since the vertical members and the buckle plate elements lie in the same plane, the stiffening effects due to composite action between the plates and the vertical

---

\* The work line is defined as the line between the contact points of the top girder which are located at the quoin and miter blocks.

members are accounted for in the moment of inertia calculations of the vertical members.

18. The location of the grid plane, which contains the skin plate and vertical members, is determined primarily by convenience and subjective judgment. This plane should be defined so as to minimize effort involved in computing the composite cross-sectional properties of the vertical beams and girders. The two recommended positions for the vertical plane would be at the skin plate or at a location that is assumed to be at the average neutral axis position of the vertical members.

19. Calculation of cross-sectional properties for composite indeterminate members involves subjective assumptions. An initial assumption must be made concerning the general structural response and the interaction between the individual components. If it is assumed that the vertical members will act relatively independent of one another, then the moment of inertia calculations should be based on the element cross section including an effective portion of the skin plate. The assumed effective skin plate width can be determined by assuming that the effective portion is that which is allowed for unstiffened elements under compression (USACE 1984). When buckle plates, rather than flat plates, are present their composite effects should probably be ignored. Conversely, if it is assumed that the vertical members will act together as a unit, the moment of inertia computations should account for the additional stiffness imposed by the eccentricity  $y$  of the member neutral axis relative to the grid plane. The effective flexural stiffness  $I_e$  of a member of cross-sectional area  $A$  can be calculated by

$$I_e = I_{NA} + Ay^2 \quad (2)$$

where  $I_{NA}$  is the moment of inertia about the member neutral axis.

20. In this case, the vertical plane should be positioned according to an average neutral axis calculation. These two methods of calculating cross-sectional properties should provide the lower and upper bounds of an element's flexural stiffness. It is likely that the true element stiffness will be somewhere between the two assumed values and can be determined through correlation with field strain data and optimization.

21. One drawback to placing the plate elements in the same plane as the vertical members is that the membrane forces due to the composite bending action of the vertical members and the skin plate are not represented by the

plate elements. This means that strains measured on the skin plate cannot be used for comparison with the analysis. In some cases, it may be necessary to produce a more realistic model in which each frame element is located according to its calculated neutral axis. Figure 1 illustrates the representation of a vertically framed miter gate using a single plane geometry.

Horizontally framed  
miter gate, simple grid model

22. A grid model is a simple approach which may also be used to represent the load transfer characteristics of a horizontally framed miter gate. Figure 2 illustrates the simple grid approximation for horizontally framed miter gates. The horizontal girders and vertical diaphragms are represented by frame elements which are located in a single bent plane (grid plane). To model the eccentricity between the horizontal girder neutral axes and the work line, the grid plane is offset near the quoin and miter ends as shown in Figure 2. Plate-membrane elements representing the skin plate are also located in the grid plane. As with the model of a vertically framed gate, the diagonal member elements are offset to their actual location using rigid links, and the most reasonable location of the grid plane is at the calculated average of the horizontal girder neutral axes.

23. The primary advantage of this approach is that it is simple to model with respect to geometry. The disadvantage is that calculations of element cross-section properties become relatively difficult, with a large degree of subjectivity. Many assumptions must be made concerning the interaction between the main structural elements and the skin plates in computing effective element stiffnesses. The same disadvantages inherent in the model of the vertically framed gate are present here. American Institute of Steel Construction (AISC) specifications (AISC 1986, 1989) provide limiting width-to-thickness ratios for effective flange widths which may be used to approximate the effective width provided by the skin plate. However, these values are design recommendations based on plate buckling requirements and are inherently conservative. An effective flange width equal to the girder spacing provides a good upper bound calculation of the girder stiffness and is likely to be more realistic. As with the vertically framed gate, an assumption must be made concerning the interaction between the girders when the neutral axis of a girder cross section is offset from the grid plane. If the girders are assumed to act independently, the moment of inertia about the girder neutral axis should be computed. However, if the girders are assumed to act as a

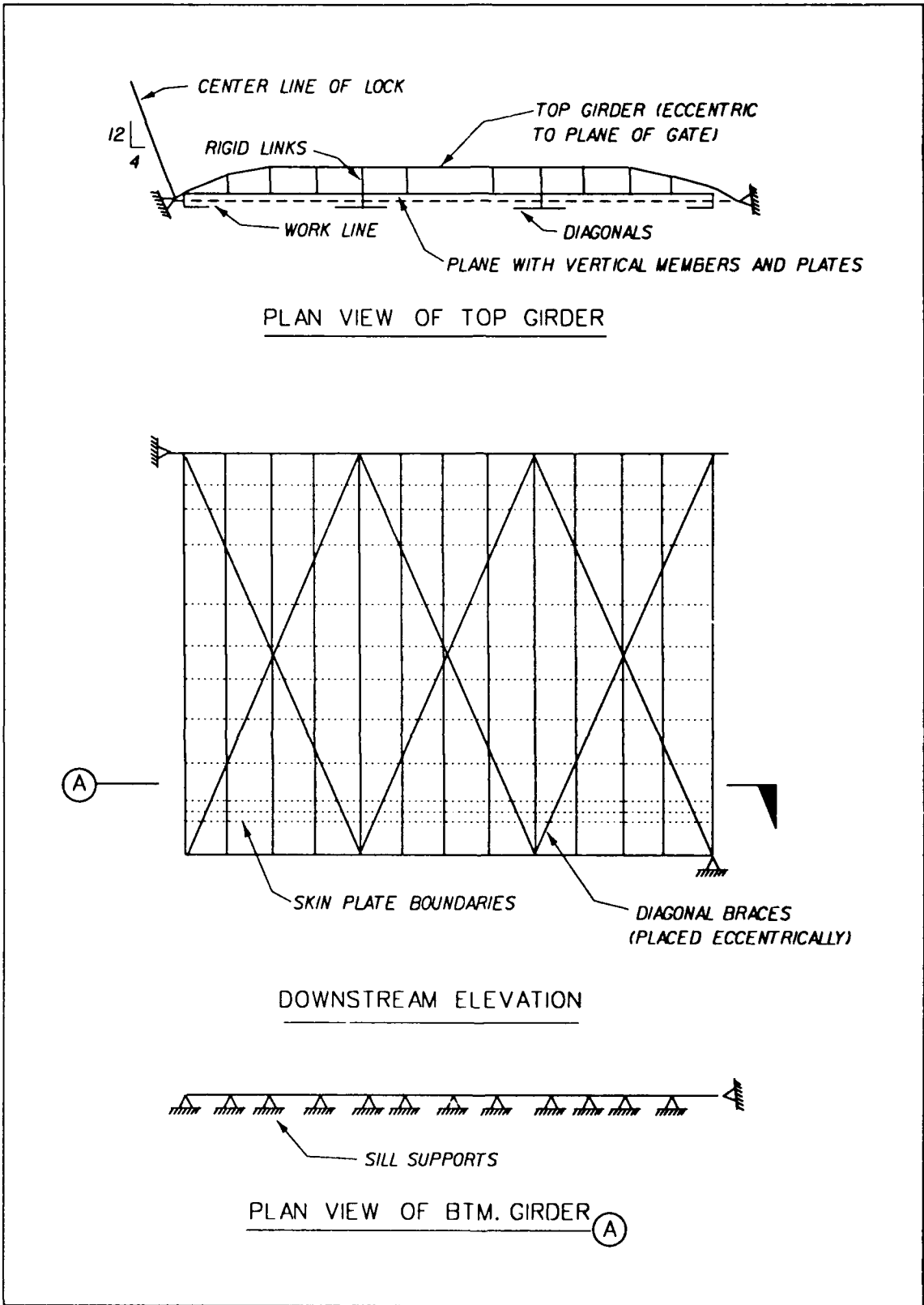


Figure 1. Representation of a vertically framed miter gate

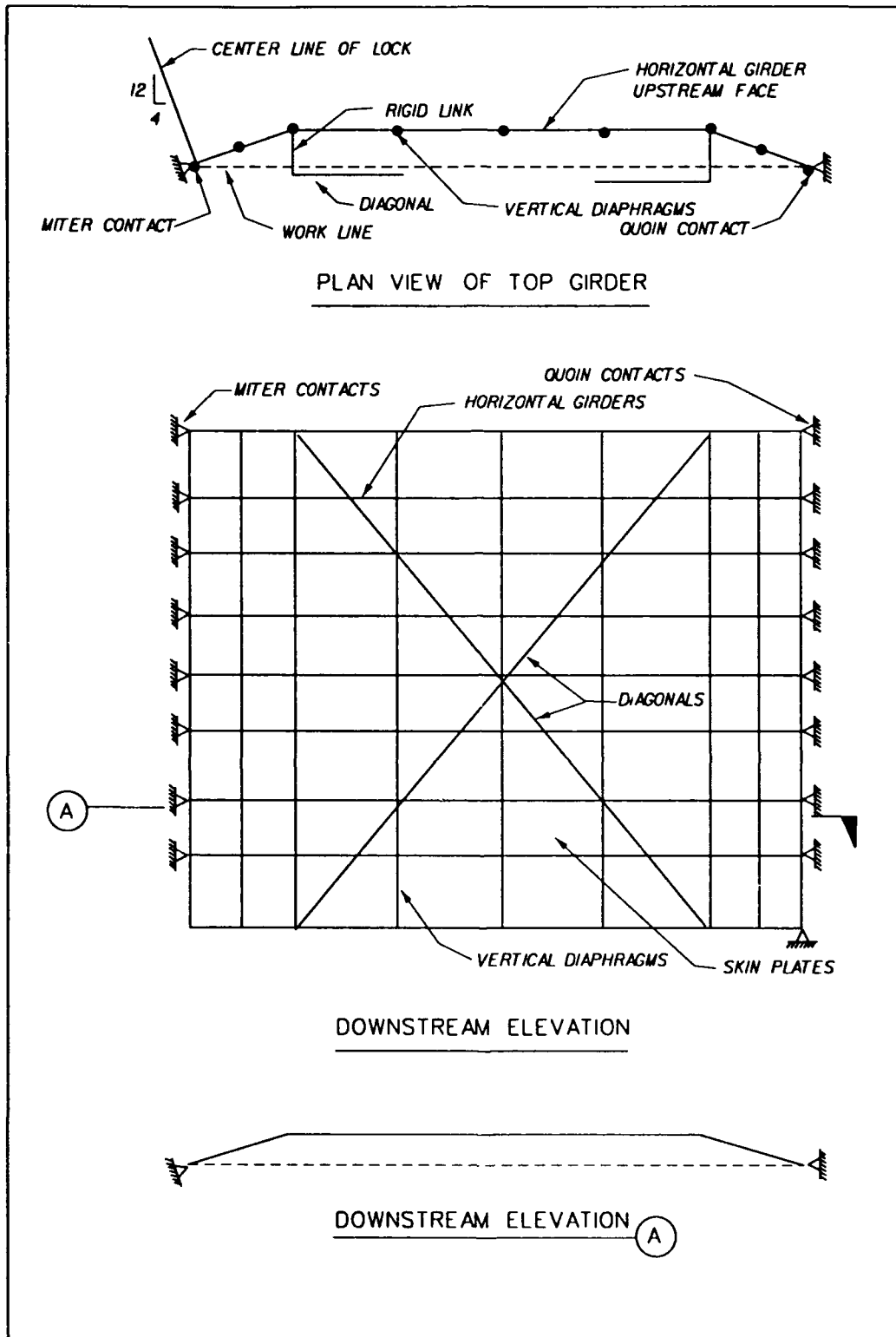


Figure 2. Simple grid model of a horizontally framed miter gate

unit, the moment of inertia of girder cross-section should be calculated about the reference plane according to Equation 2.

24. Another consideration in determining cross-section properties is that the cellular construction of the gate leaves tends to significantly increase the torsional stiffness of the main structural members by providing resistance against warping in the girder and diaphragm flanges. Therefore, warping constants must be implemented in the frame elements and assumptions must be made concerning the effects the skin plate has on the warping torsion. If the gate is represented in the miter position or if the majority of torsional strength of the gate is assumed to be provided by the diagonal members, then the problem of torsional stiffness in the frame elements is of little importance.

25. As with the model of the vertically framed miter gate, calculated strains in the skin plate are typically inaccurate since the membrane forces due to composite bending are not represented by this geometry.

Horizontally framed  
miter gate, refined grid model

26. The refined grid model which includes a more accurate representation of structure geometry compared to the simple grid model is illustrated in Figure 3. It is composed of the same grid plane as that of the simple grid model with the exception that the skin plate elements are offset from the grid with rigid links to better represent the depth of the gate. As with previously described models, the diagonal member elements are offset to their actual location using rigid links. By using this representation, the composite behavior of the frame elements and the skin plate is accounted for explicitly. The effective increase in flexural member stiffness due to composite action is accounted for by the membrane action of the plate elements. Therefore, it is not required to include the effect of the skin plate in the frame element moment of inertia calculations and the calculated strains in the skin plate should be more accurate than in the simple grid approach. This approach includes a more accurate representation of geometry than the simple grid approach but requires a significant increase in the number of nodes. The number of nodes in the model is approximately doubled so the amount of data input and the computer run time are both significantly increased.

27. The calculation of girder and diaphragm cross-sectional properties is simplified since the effects of the skin plate do not need to be included in the element stiffness computations; however, defining the location of the

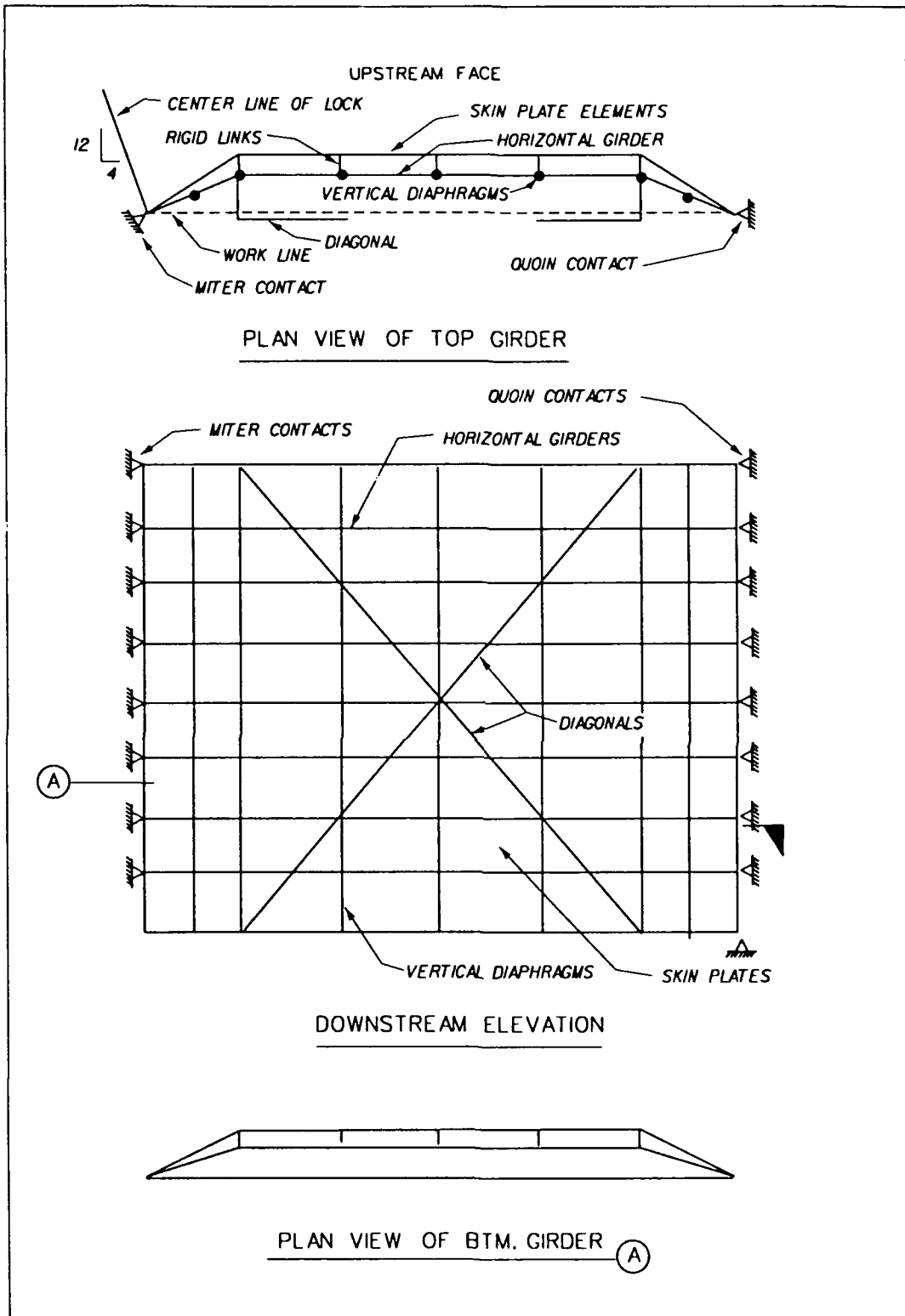


Figure 3. Refined grid model for a horizontally framed miter gate

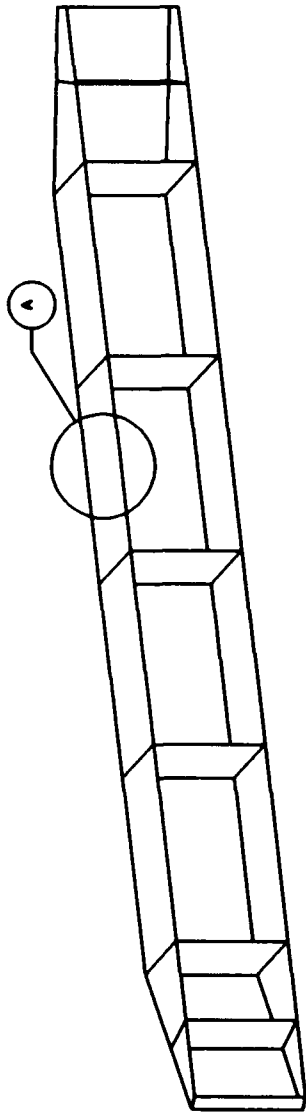
grid plane still requires some assumptions. Although several viable alternatives exist, the calculated average of girder neutral axes is the recommended choice for the grid plane location. For members with neutral axes eccentric to the grid plane location, the eccentricity should be accounted for in the flexural stiffness computations. Thus, the overall accuracy of the refined grid model may not be significantly improved when compared to the simple grid model.

28. As with the simple grid model, warping torsion constants must be implemented in the frame elements. Since the skin plates are offset from the frame elements, their effect on the torsional stiffness of the girders and diaphragms should already be taken into account.

Horizontally framed miter gate,  
refined three dimensional (3-D) model

29. Another approach to simulating horizontally framed miter gates is to model the flanges and webs of each girder and diaphragm separately. For each girder and diaphragm, member flanges are represented by frame elements and plate-membrane elements are used to simulate the web. The skin plate elements are connected to the flange nodes on the upstream face of the gate. The refined geometry greatly simplifies the calculation of section properties for the primary structural elements. The moment of inertia about each axis, the cross-sectional area, St. Venant's torsion constant, and the warping factor are all implicitly defined by the geometric configuration and the elementary properties assigned to the flange and web members. Figure 4 illustrates the concept of modeling girders with frame and plate-membrane elements. It is apparent that the actual shape of the structure is more closely represented with this approach than in the two previously mentioned grid models.

30. The main disadvantage of this model is the complexity in defining the nodal positions and element connectivity. The number of nodes required is approximately the same as for the refined grid model, but the number of frame elements approximately doubles and the number of plate-membrane elements increases by a factor of about three. Thus, user input, computer memory requirements, and run times increase significantly. Implementation of this modeling procedure would likely approach the memory limitations of most personal computers. It is expected that memory requirements for most miter gate models of this type would be between 4 and 8 megabytes.



3-D MODEL OF TWO GIRDERS

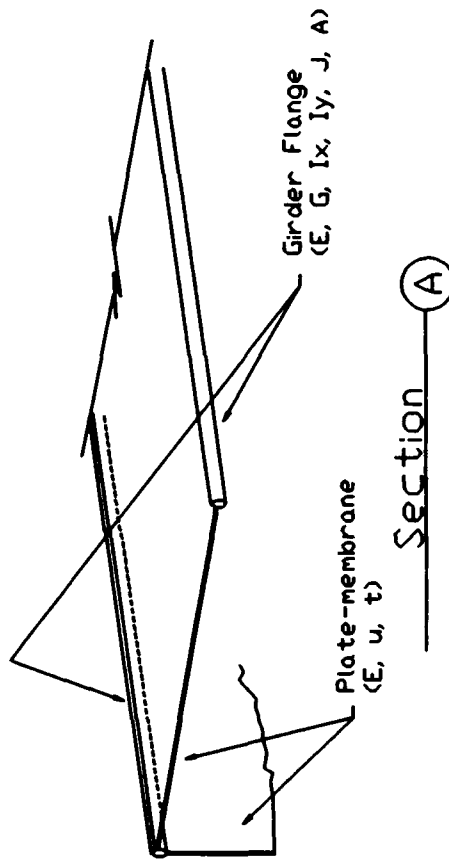


Figure 4. 3-D representation of two horizontal girders

### PART III: CASE STUDIES

31. To aid in development of the modeling and analysis procedures as applied to lock gates, two case studies were performed. The first case study involved a vertically framed miter gate. Experimental data were available for a barge impact test conducted on the lower vertically framed miter gate at the old Lock and Dam 26 north of St. Louis, MO. The test was destructive in the area of impact. However, strains measured at other points on the structure provided a reasonable basis for comparison since the global behavior was elastic (Chasten and Ruf 1991).

32. A second case study was conducted for a horizontally framed gate. A single measurement of leaf dead load displacement was available for a gate leaf at the John Hollis Bankhead Lock and Dam near Birmingham, AL (Emkin, Will, and Goodno 1987). This measurement was used to indicate the suitability of the modeling procedures for dead load response of horizontally framed miter gates. In the following paragraphs, each of these case studies is discussed in detail.

#### Lock Gate 26, Mississippi River

33. The old Mississippi River Locks and Dam 26, located just north of St. Louis was recently replaced by the Melvin Price Lock and Dam. Prior to demolition of the old locks, destructive impact tests were performed on the downstream gate of the main lock (Goble, Schulz, and Commander 1990b). The gate which was tested was a vertically framed miter gate. During the impact tests the gate was in the miter position and no head differential was present. The impact load was applied by a moving nine-barge tow in four separate occurrences. During each test, strain data were recorded at 27 locations on the miter gate along with the impact force, barge velocity, and barge acceleration. Symmetry of load transfer was verified by nearly equal strain measurements at similar locations on both gate leaves.

34. Data from these tests provided a basis for developing and evaluating analysis modeling techniques for vertically framed miter gates. Various approaches in representing the gate leaf were attempted, starting with a very simple planar grid model in which all elements were defined within a single vertical plane. Modifications to the model were implemented until a reasonable correlation between analytical and experimental results was reached. The

process of geometry modification was one of trial and error and progressed as the understanding of miter gate performance improved. In the development of the selected model, it was apparent that the frame elements representing the top girder should be located as close as possible to the neutral axis of the top girder. This is necessary since the eccentricity between the line of action of the axial load (work line) and the girder neutral axis results in a substantial bending moment in the top girder. The model which was finally selected consisted of the geometry discussed in Part II, "Vertically framed miter gate."

35. Since the response of the gate leaves in the impact test was symmetric, only one gate leaf was modeled. A concentrated load equal to one half of the measured impact load was applied to the miter girder at the point of contact. Computations for the top girder cross-sectional properties were based on the girder web and flanges only (effect of skin plate was not included). The eccentricity of the top girder elements with respect to the work line induced the appropriate bending moment and axial force responses in the top girder. A small fraction of the top girder axial resultant force was assumed to be carried by the skin plate. To accurately model this effect, it was determined that the grid plane (containing the buckle plate elements and vertical member elements) should be located at the center line of the buckle plates. However, this procedure may not be the most appropriate for other load conditions which induce substantial flexure in the vertical members. Rigid link elements were used to space the top girder and the grid plane appropriately, and to maintain continuity between the top girder and the other structural components. The miter and quoin contact points were located at the ends of the top girder. Since the vertical beams and girders lie in the same plane as the plate elements, the stiffening effect of composite action between the plate and the vertical beams was taken into account in the moment of inertia calculations of the vertical members. However, the flexural stiffness of the vertical members had little influence when considering this loading situation (no differential head).

36. The final model was obtained when the correlation of the general responses was assumed to be accurate, and most results were within 20 percent of the field measurements. All modifications performed were based strictly on geometry changes. No parameter optimization was performed, as the goal for this phase of the project was to obtain general modeling characteristics

rather than structural parameter evaluation. Also, there was no visible deterioration or any reason to justify alteration of structural parameters.

#### Model details

37. A description of the analysis and modeling details is presented here, and a listing of the SAC input data is provided in Appendix C. The final model consisted of 211 nodal points which translates into 1266 degrees of freedom minus those eliminated by the boundary conditions. There were 234 space frame elements and 56 rectangular plate-membrane elements. Twenty different element groups were required to define the cross-sectional and material properties of all the structural elements. All of the material properties for structural elements were based on assuming 36-ksi\* steel. Rigid link elements were used to connect the top girder and diagonal elements to the rest of the structure. These elements were assigned extremely large axial, bending, and torsional stiffnesses as compared to the main structural elements and are considered to act in rigid manner.

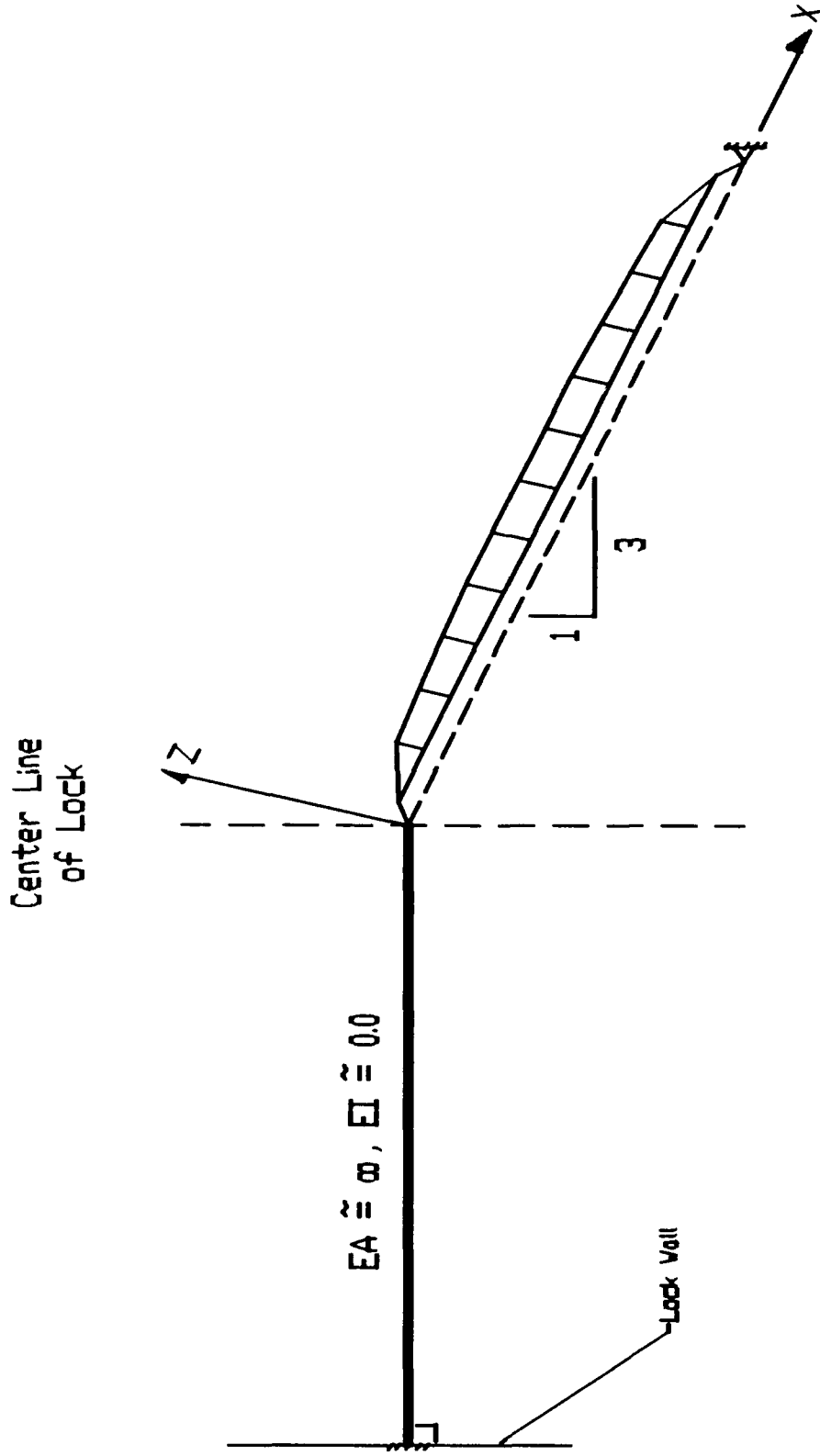
38. Since symmetry was assumed, only one gate leaf was defined and the action of the other gate was simulated with an effective inclined roller support at the miter contact point. Inclined roller supports cannot be defined in SAC since boundary conditions are defined in global coordinates only. Thus, a bar element aligned normal to the desired inclined roller plane was used to simulate the roller support. The bar element was given axially rigid properties but had no bending or torsional stiffness. One end of the bar element was fixed and the other was located at the miter contact point. To assure that translation of the contact point could only occur along the inclined plane, the bar element was defined with a substantial length, approximately equal to that of the entire miter leaf. To illustrate this modeling concept further, a plane view of the top girder and the inclined roller support is presented in Figure 5. This procedure for obtaining symmetry can be applied to horizontally framed gates, regardless of the geometric complexity.

#### Result comparisons

39. Analysis results from the final model were compared with field test results at several locations on the lock gate. Experimental strain

---

\* A table of factors for converting non-SI units of measurement to SI (metric) units is presented on page 4.



PLAN VIEW OF TOP GIRDER & MITER CONTACT

Figure 5. Representation of roller supports to model symmetry

measurements were used to calculate the axial force and flexural moment for specific element cross sections. The emphasis on the comparisons was based on responses of the top girder since it was responsible for transferring the majority of the impact load to the lock walls. The experimental results and corresponding analytical results are presented in Tables 1-4. The results are presented for two values of impact magnitude for each of the four events. Table 1 includes strain responses, corresponding to locations shown by Figure 6, for the middle of the top girder. The strain comparisons on the web at this section may not be very accurate as there was a large hole in the web of the girder near the instrumentation. A comparison of axial force and bending moment at the center of the top girder is provided in Table 2. Tables 3 and 4 contain the axial force and moment comparisons near the miter and quoin ends of the top girder. Strain measurement devices (transducers) were placed at approximately the quarter points of the top girder as illustrated in Figure 6.

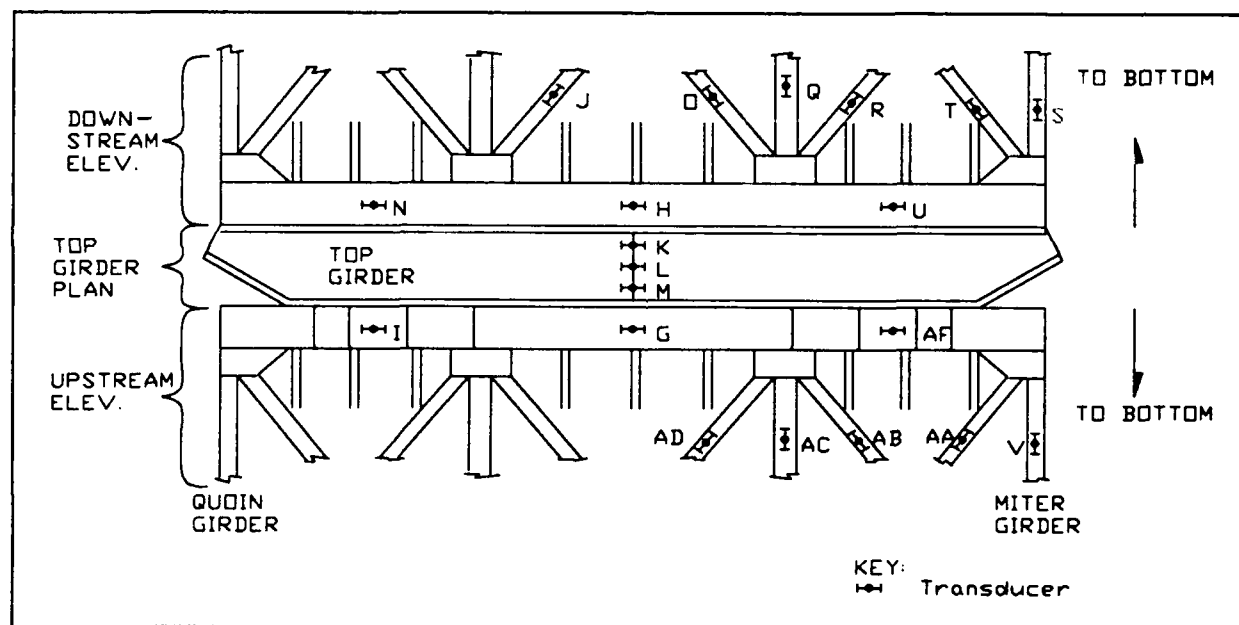


Figure 6. Transducer locations on top girder

#### Case study conclusions

40. The primary conclusion that was drawn from this study is the basic analysis and modeling procedures are appropriate for obtaining reasonably accurate predictions. Based on the tabulated results, it is apparent that most of the calculated responses are within 20 percent of the measured results. Considering the assumptions involved in modeling and in calculating experimental force resultants, this can be considered a good correlation. The

Table 1  
Strains at Top Girder (Center Cross Section)

Impact Number	Impact Load (kips)	Strain (in./in. $\times 10^{-6}$ )									
		H		K		L		M		G	
		F*	A*	F	A	F	A	F	A	F	A
1 (max)	442.9	-386	-302	-109	-201	-99	-109	-76	-53	-8	-1
(=75%)	350.0	-313	-239	-81	-159	-67	-86	-48	-42	-3	-0.8
2 (max)	443.6	-386	-303	-122	-201	-105	-109	-65	-53	15	-1
(=75%)	344.2	-293	-235	-83	-156	-70	-85	-43	-41	5	-0.8
3 (max)	604.7	-587	-412	-144	-274	-141	-149	-96	-72	-16	-1
(=75%)	453.2	-347	-309	-92	-206	-82	-112	-61	-54	-5	-1

\* F = field, A = analysis.

Table 2  
Axial Force and Flexural Moment, Top Girder Center

Impact Number	Impact Load (kips)	Axial Force (kips)			Bending Moment (kip-ft)		
		Field	Analysis	% Error	Field	Analysis	% Error
1 (max)	442.9	-432.2	-371.52	-14.04	1173.0	1019.9	-13.05
(=75%)	350.0	-331.6	-293.6	-11.46	968.3	806.0	-16.76
2 (max)	443.6	-396.7	-372.1	-6.20	1266.3	1021.5	-19.33
(=75%)	344.2	-302.2	-288.7	-4.47	937.9	792.6	-15.49
3 (max)	604.7	-640.9	-507.2	-20.86	1771.4	1392.5	-21.39
(=75%)	453.2	-377.1	-380.2	0.82	1061.6	1043.6	-1.70

Table 3

Axial Force and Flexural Moment, Top Girder Miter End

<u>Impact Number</u>	<u>Impact Load (kips)</u>	<u>Axial Force (kips)</u>			<u>Bending Moment (kip-ft)</u>		
		<u>Field</u>	<u>Analysis</u>	<u>% Error</u>	<u>Field</u>	<u>Analysis</u>	<u>% Error</u>
1 (max)	442.9	-509.0	-402.9	-20.84	1160.0	1114.9	-3.89
(=75%)	350.0	-377.5	-318.4	-15.66	914.7	881.1	-3.67
2 (max)	443.6	-379.8	-403.5	-6.24	1382.0	1116.7	-19.20
(=75%)	344.2	-360.7	-313.1	-13.20	1145.5	866.4	-24.36
3 (max)	604.7	-1621.4	-550.1	-66.07	3989.9	1522.2	-61.85
(=75%)	453.2	-1399.9	-412.3	70.55	3580.7	1140.8	-68.14

Table 4

Axial Force and Flexural Moment, Top Girder Quoin End

<u>Impact Number</u>	<u>Impact Load (kips)</u>	<u>Axial Force (kips)</u>			<u>Bending Moment (kip-ft)</u>		
		<u>Field</u>	<u>Analysis</u>	<u>% Error</u>	<u>Field</u>	<u>Analysis</u>	<u>% Error</u>
1 (max)	442.9	-446.4	-426.6	-4.44	1123.0	919.2	-18.15
(=75%)	350.0	-363.0	-337.1	-7.13	873.2	726.4	-16.81
2 (max)	443.6	-414.2	-427.3	3.16	1177.5	920.7	-21.81
(=75%)	344.2	-332.7	-331.5	-0.36	829.7	714.4	-13.90
3 (max)	604.7	-705.1	-582.5	-17.39	1743.9	1255.0	-28.03
(=75%)	453.2	-428.3	-436.8	1.98	1039.7	940.6	-9.53

results were better at locations away from the miter end since there was yielding near the impact point (see Table 3, impact 3).

41. It was previously noted that the final model was obtained by modifying the model geometry to obtain the desired accuracy. All section parameters were computed using basic principles of mechanics of materials and no parameter optimization was performed. It is assumed that these parameters are reasonably accurate since the lock gate showed no signs of significant deterioration. One structural parameter, the torsional resistance of the frame elements, may not be highly accurate and may require optimization when other loading conditions such as dead load, water loading, or gate operation are applied. Beam torsion constants were obtained from the basic equation of nonrestrained thin-walled open sections ( $\Sigma h_i t_i^3/3$ ). For loading situations when element torsion is significant, it is likely that restrained warping torsion will need to be accounted for. Lock gate geometry is such that girder and diaphragm flanges are usually restrained against warping which significantly increases torsional stiffness of the gate. Restrained warping torsion can be modeled by either applying warping constant terms in the torsional stiffness calculations of the frame elements, or by using a refined 3-D geometry in which the flange warping is simulated by the additional degrees of freedom.

#### John Hollis Bankhead Lock and Dam

42. The John Hollis Bankhead Lower Miter Gate on the Black Warrior River in Alabama was the subject of a finite element study on horizontally framed miter gates (Emkin, Will, and Goodno 1987). Reports generated from this study were reviewed to obtain general modeling procedures and were used to provide a basis for analysis evaluation. A single field measurement was obtained from this study and was used as the validation criteria for the adopted modeling techniques. An out-of-plumb displacement of the gate leaf due to gravity loading only was taken prior to the attachment of the diagonal braces. It was assumed that it was not a highly accurate measurement as residual and fabrication stresses alone could account for a considerable amount of warping in the gate leaf. It was desirable, however, to obtain results in the same order of magnitude.

43. Since the dead load acts at the structure center of gravity which is eccentric from the structure shear center (indicated by the out-of-plumb

displacement), the refined grid model was selected as the appropriate geometry configuration. The simple grid model was not capable of accurately representing the eccentricity of the dead load, and the 3-D model was considered too involved to utilize without the aid of automatic mesh generation and was therefore not attempted.

#### Model development

44. Miter gate details were obtained from contract drawings and a numerical model of one leaf was developed using the refined grid approach outlined in Part II (Figure 3). The girders and diaphragms were simulated by frame elements and the skin plate was simulated using rectangular plate-membrane elements. To account for the eccentricity between the skin plate and neutral axis of the girders and diaphragms, rigid links were utilized to offset the skin plate in a realistic manner. The girder and diaphragm frame elements were located at the position of the center of area of the girders. This location was selected so the load due to structure weight would be positioned appropriately. Boundary conditions were applied at the pintle and gudgeon pin locations and an additional support was added to the bottom girder simply to maintain a stable structure (i.e. keep the gate leaf from swinging). Gravity loads were automatically calculated and applied by providing the unit weight of steel.

45. The out-of-plumb field measurement (Emkin, Will, and Goodno 1987) was the horizontal displacement of the top miter corner relative to the bottom miter corner and was equal to 4.75 in. Results from the first analysis run indicated an out-of-plumb displacement of 44.7 in. which is in error by a magnitude of about 10.

46. It was determined that much of the error was due to the extremely low torsional stiffness values given to the frame elements. The torsion constants were computed for thin-walled open sections subject to St. Venant's uniform torsion, in which all of the torsion is resisted by the shear stress in the cross-section walls and resistance due to warping is neglected. However, the cellular construction of the gate leaf induces a considerable amount of resistance to flange warping. The consideration of restrained warping in the flanges increases the overall torsional stiffness of the horizontal girders by a factor of about 20. Therefore, the model was modified to incorporate warping constants of element cross sections in the torsional stiffness terms. A discussion of warping torsion as it pertains to the analysis is presented in Appendix D.

47. The warping constants were computed for each frame element cross section and entered in the input file. The new analysis resulted in an out-of-plumb displacement prediction of 18.6 in. which was a considerable improvement over the initial results. Implementing the restrained warping torsion terms in the model significantly increased the torsional stiffness of the gate leaf and reduced the error to a magnitude of 4, but this was still regarded as unacceptable.

48. Further examination revealed a modeling deficiency in the rectangular plate-membrane elements. As discussed in Part II, "Structural geometry and element library," the hybrid plate-membrane elements are composed of two separate elements: (a) a rectangular Kirchhoff plate element that resists an out-of-plane displacement and rotations about the two in-plane axes, and (b) a plane strain quadrilateral membrane element that resists displacements in the two in-plane axes. The resistance of each of the components is uncoupled due to the small displacement assumption. The combined stiffness terms in the plate-membrane element account for only five degrees of freedom at a given node as shown by Figure 7(A), and the plate-membrane element does not include a stiffness term for the sixth degree of freedom (rotation about the out-of-plane z-axis). This degree of freedom corresponds to that of the bending stiffness about the weak axis of the attached frame elements which influences the overall gate leaf torsional resistance. Hence, by neglecting the sixth degree of freedom in the plate-membrane element, the numerical representation of the gate leaf is too flexible when torsional resistance is a factor. Figure 7(A) illustrates the degrees of freedom resisted by the plate-membrane element, and the modeling deficiency as it applies to this application is shown in Figure 7(B).

49. To remedy this situation, two possible solutions exist. The first is the development and implementation of a new plate element which contains the stiffness terms for the sixth degree of freedom. The second approach would be to refine the mesh (reduce size of plate-membrane elements) as shown in Figure 8 so that the in-plane resistance of the plate elements would be effective in resisting weak axis bending of the attached frame elements. These options were not considered to be feasible within the scope of this project and since the deficiency was not deemed relevant to the majority of load conditions they were not pursued.

50. Adding the sixth degree of freedom stiffness terms to the skin plate elements would effectively increase the lateral (weak axis) stiffness of

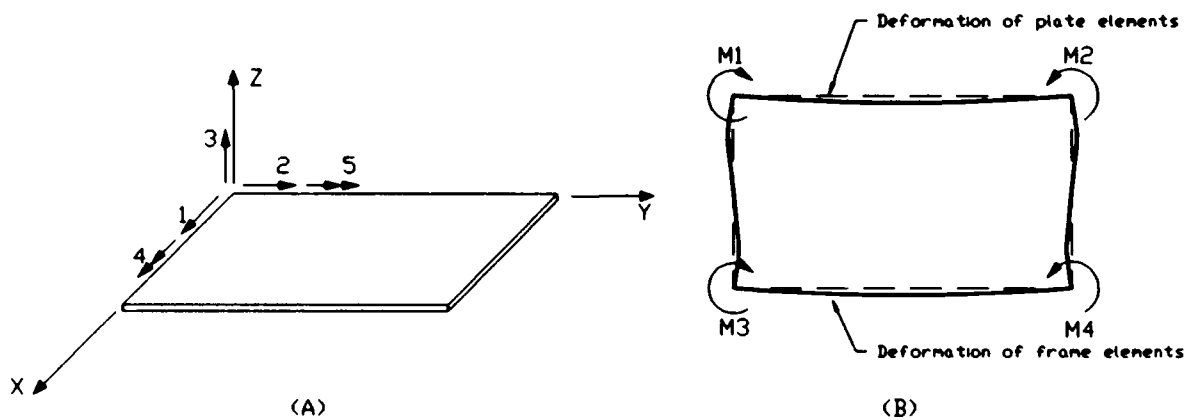


Figure 7. (A) Degrees of freedom associated with plate-membrane element  
 (B) Modeling deficiency due to missing rotational stiffness terms

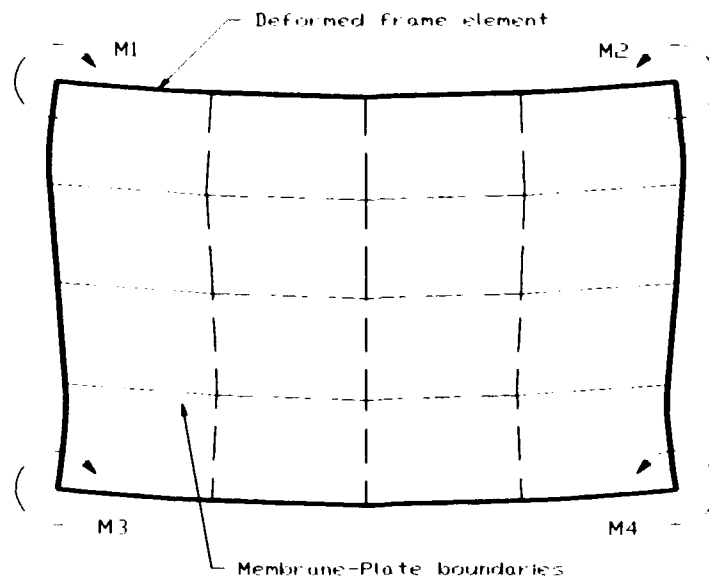


Figure 8. Mesh refinement approach to modeling in-plane bending

the elements representing the horizontal girders, diaphragms, and the quoin and miter girders. Therefore, it was of interest to determine the effect of increasing the lateral stiffness of the frame elements. Although the procedure may be purely academic, it was assumed that an effective flange width of 4 ft (spacing between the lower horizontal girders) could be contributed by the skin plate. The moments of inertia about the weak axes were then

recalculated using this assumption. Reanalysis using the modified input data resulted in an out-of-plumb displacement of 3.1 in., which was well within the desirable error limit.

51. It may be argued that some of the skin plate effects were now being applied to the gate leaf twice, increasing the gate stiffness by an unrealistic amount. As a means of determining the effect that the skin plate elements have on the torsional stiffness of the gate leaf, the modulus of elasticity in the skin plate elements was set to zero and the analysis was again performed. The result was the plate-membrane elements had very little effect, as the new displacement result was evaluated at 4.9 in. Compared with the field measurement of 4.7 in., this was considered to be adequate. Even though the lateral stiffness properties applied to the model cannot be considered accurate, the general effect of the modeling deficiency in the plate-membrane elements was verified.

#### Case study conclusions

52. Evaluation using the out-of-plumb displacement (measured with diagonals not attached) is generally not relevant to miter gate performance as the majority of torsional stiffness is provided by the diagonals and the torsional rigidity is a minor consideration when the gate is in the miter position. Dead load deflections will generally not be obtainable for existing structures because the diagonals are already in place, so the use of the refined grid model may not be necessary. Since most loading is applied normal to the plane of the gate, this measurement should not be the sole means of evaluating the modeling procedures, yet it does provide some insight as to the suitability of the numerical model. An extremely good correlation was achieved with the refined grid approach, although some of the obtained cross-sectional properties cannot be completely rationalized. If it is determined that this type of load response is important, then the 3-D model would be the best approach since the independent modeling of the beam flanges more realistically depicts the warping torsion problem. A new membrane element, capable of resisting rotation about the out-of-plane axis (sixth degree of freedom), would also need to be developed and implemented to obtain a realistic overall torsional stiffness.

#### PART IV: GENERAL CONCLUSIONS

53. The approach of modeling and modifying the structural parameters has been tested with a high level of success on highway bridges (Goble, Schulz, and Commander 1990a and Goble et al. 1991). Based on these initial case studies, it is apparent that it is applicable to miter gates as well. The level of field verification to date is limited and a considerable amount of experimental testing is still required. The tools developed so far are sufficiently refined to proceed with prospective case studies; however, it is assumed that modifications to modeling procedures may be necessary, pending comparisons with future field tests. The analysis program can be modified as required to implement new modeling capabilities.

54. Since field verification is very limited, a clear decision regarding the best modeling procedures cannot be made at this time. It is proposed that specific model geometries will be selected based on correlations made with field tests which are scheduled for future phases of this project. Conclusions made at this time are mainly qualitative and subject to change.

##### Vertically Framed Miter Gates

55. Based on this initial study, the only modeling procedure presented for vertically framed miter gates is that of the simple model. However, as in the case for horizontally framed miter gates, a 3-D model may be required for detailed analyses for certain loading conditions such as those which cause gate leaf twist.

##### Horizontally Framed Miter Gates

56. The refined grid model was selected for the horizontally framed gate leaf modeled in the second case study. This was due to the nature of the gravity load response and the single available displacement measurement. Typically, this load response will be of little consequence so that the use of the refined grid model may not be the best alternative. When considering model generation, the refined grid model is considerably more complicated than the simple grid model and there is little overall benefit. For most applications, the major advantages of the refined grid are that the theoretical strains in the plate will be more realistic and the composite action of the

skin plate does not need to be considered in the calculation of the horizontal girder properties. The same assumptions regarding the location of the frame elements must be applied in both the simple and refined grid models, so a significant improvement in accuracy may not be achieved by using the refined grid model. Requiring a fraction of the modeling effort and computer run time, the simple grid geometry is generally the preferred modeling approach. The primary disadvantage of the simple approach is in the computation of effective element stiffness values as discussed in Part II, "Vertically framed miter gate." When a more sophisticated representation is required such as prediction of gate twist, it would then be beneficial to implement the 3-D geometry since it is significantly more realistic than either of the grid models.

## PART V: FUTURE IMPLEMENTATIONS

57. Regardless of the model geometry selected, an interactive preprocessor which aids in rapid development and modification of miter gate finite element meshes is required to make routine analysis feasible. Graphical representation of structure geometry, load conditions, and structural responses would reduce the number of user input errors and aid in the detection of gross errors in geometry and boundary conditions. A visual display of measured and calculated responses would also provide intuitive insight to lock gate responses. It is intended to develop software with these capabilities during future phases of this project.

58. The comparisons of experimental and analytical data have thus far indicated that SAC can provide accurate representation of miter gates. However, the field data at this stage are rather limited. To fully verify the modeling and analysis procedures, data comparisons for a variety of lock gates and load configurations are recommended.

59. Through the John Hollis Bankhead Lock Gate study, it was observed that a modeling deficiency exists in the plate-membrane elements currently utilized by the analysis software. This deficiency is assumed to be a minor consideration, generally; however upon further field verification, the implementation of a refined membrane element may be substantiated.

60. Due to various eccentricities and member neutral axis locations, determining flexural stiffness constants for the horizontal or vertical girders and selecting appropriate locations for the grid plane is a common problem in the development of each grid model. Using the current models, elements for members which actually have different locations must be located in a common plane. This is required to make generation of the models feasible and to maintain continuity at nodal points with multiple elements attached. A relatively simple approach to eliminating this problem would be to modify the analysis program so that eccentricity terms are included in the individual element stiffness matrices. The resulting benefit is that a common reference plane could be used to define the entire structure, yet each element could have a unique location. This would essentially provide the same effect as using rigid links to connect an element to the plane, but additional nodes and elements would not be required. Implementation of the eccentricity terms would be relatively simple since they can be applied through transformation matrices. An example of this type of element is shown in Figure 9.

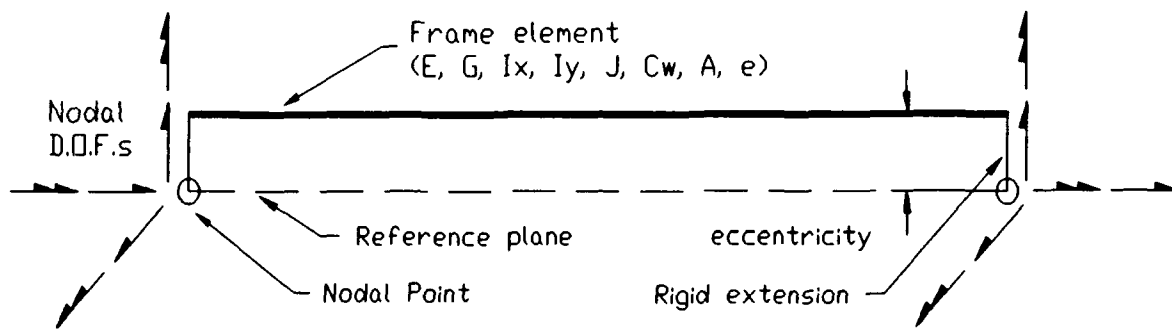


Figure 9. Frame element with built-in eccentricity term

## REFERENCES

- American Institute of Steel Construction. 1986. *Manual of Steel Construction, Load and Resistance Factor Design (LRFD)*, 1st ed., Chicago, IL.
- \_\_\_\_\_. 1989. *Manual of Steel Construction, Allowable Stress Design (ASD)*, 9th ed., Chicago, IL.
- Chasten, C. P., and Ruf, T. 1991. "Miter Gate Barge Impact Testing, Locks and Dam 26, Mississippi River," *Proceedings of the 1991 Corps of Engineers Structural Engineering Conference*. (Proceedings in preparation)
- Emkin, L. Z., Will, K. M., and Goodno, B. J. 1987. *Finite Element Studies of a Horizontally Framed Miter Gate*, Technical Report ITL-87-4, US Army Engineer Waterways Experiment Station, Vicksburg, MS.
- Frangopol, D.M., and Klisinski, M. 1989. "Material Behavior and Optimum Design of Structural Systems," *Journal of Structural Engineering, ASCE*, Vol 115, No. 5, p 1054.
- Goble, G. G., Schulz, J. X., Commander, B. C. 1990a. *Simple Load Capacity Tests for Bridges to Determine Safe Posting Levels: Final Report*, submitted to the Pennsylvania Department of Transportation by the Department of Civil and Architectural Engineering, University of Colorado, Boulder, CO.
- \_\_\_\_\_. 1990b. *Lock and Dam #26 Field Test Report for the Army Corps of Engineers*, submitted by Bridge Diagnostics, Inc., Boulder, CO.
- Goble, G. G., Schulz, J. X., Commander, B. C., Burgess, C. U., Dow, J. O., and Frangopol, D. M. 1991. *Load Prediction and Structural Response: Final Report*, submitted to the Federal Highway Administration by the Department of Civil and Architectural Engineering, University of Colorado, Boulder, CO.
- Robson, B. 1990. "Predicting Structural Response in Highway Bridges," M.S. Thesis, University of Colorado, Boulder, CO.
- Rosenbrock, H. H. 1960. "An Automated Method for Finding the Greatest or Least Value of a Function," *Computer Journal*, Vol 3, p 175.
- US Army Corps of Engineers. 1984. *Engineering and Design, Lock Gates and Operating Equipment*, Engineer Manual 1110-2-2703, Washington D.C.
- \_\_\_\_\_. 1988. *The 1988 Inland Waterway Review*, Institute for Water Resources, Ft. Belvoir, VA.

## APPENDIX A: PARAMETER OPTIMIZATION

1. The unique feature of *SAC* is its ability to compare certain analysis results with a corresponding set of data and to modify structural parameters so as to obtain the best correlation. This feature was developed to provide a means of evaluating various parameters that cannot be well defined. Parameter modification is performed using a constrained optimization technique, in which the user can specify what structural parameters are to be optimized. The process is considered constrained since the optimized values must fall within user specified limits. Parameters which can be optimized are the material stiffnesses and cross-sectional properties for each user defined element group.

2. Variable optimization is performed by an iterative process in which the goal is to minimize a single objective function. The objective function is defined as the sum of the absolute differences between the analysis results and the corresponding test data. The structural response used to calculate the objective function is strain at selected experimental gage locations. The absolute value of the strain difference is computed at each gage location and then summed to form the objective function. Thus any differences in the theoretical and experimental strain values will always result as an increase in the objective function. The goal of the optimization is to then minimize this error function. Once the analysis is run and the error value is defined, the specified parameters are systematically altered and the analysis is run again. The new error is compared with the previous value and it is determined if the correlation improved. This iterative process is continued until an acceptable correlation (i.e. an error of less than one percent of the total absolute measured strain) is obtained or until a maximum number of iterations are reached. If an acceptable correlation cannot be achieved, this indicates that the model is not an appropriate representation of the actual structure.

3. The optimization process used in *SAC* is a "constrained, direct search method for a single-objective minimization algorithm." This algorithm was developed by Frangopol and Klisinski (1989)\* and is an extension of the method of unconstrained minimization by Rosenbrock (1960). The integration of

---

\* See REFERENCES at end of main text.

this process with an analysis program was first performed during a study sponsored by the Federal Highway Administration (Robson 1990).

4. Care must be taken in selecting appropriate positions for strain comparisons. The locations for which strain is to be compared are essentially dependent on the information sought, or the variables that are considered to be unknown. In general, the number of strain values should be equal to or greater than the number of unknown quantities. Locations should be selected so that strain responses at that point will be directly affected by the value of an unknown parameter. Assorted load configurations can also be used to obtain additional strain comparisons.

5. When optimizing various structural parameters, it is important to avoid optimizing two or more variables that are directly correlated or have identical effects on the structural response. For example, the flexural stiffness of a girder is dependent on the product of the material modulus of elasticity  $E$  and the moment of inertia  $I$ . These two parameters cannot be optimized at the same time if stiffness is of concern since they have identical effects on the response. While attempting to optimize the flexural stiffness of a beam, one term might approach infinity and the other term might approach zero. Another important factor in the optimization process is the constraints on a given parameter. The upper and lower limits should be defined using good engineering judgment. If a parameter is to be optimized it is necessary that the range be sufficiently broad so that it will have a measurable effect on the response. However, since the step size of a parameter change is based on a percentage of the total range, it is necessary that the variable have realistic boundaries.

6. The ability of the program to obtain a good correlation is dependent on the quality of the model and the relevance of the unknown parameters to the measured response. The number of iterations required to reach the desired correlation is directly proportional to the number of parameters being optimized. It is desirable to keep the selected unknown variables to a minimum as it reduces the computer run time and it generally improves the correlation. Fewer strain comparison locations are required if the number of optimized variables is reduced.

7. This method of incorporating an optimization algorithm within a structural analysis program to evaluate structural models is a relatively new

concept. In the current version of *SAC*, a rather simplistic process was implemented to determine if the concept was feasible. Thus far, the approach has achieved good results, so it may be desirable to adopt a more sophisticated optimization algorithm. More complex minimization techniques exist that may improve the convergence time and correlation of the models with their respective experimental data.

## APPENDIX B: COMPUTER IMPLEMENTATION

1. Even though it is desirable to keep miter gate models simple, it is possible that some numeric representations will be relatively large compared to most PC applications. To maintain the use of SAC on a PC, several features have been incorporated to minimize memory requirements and maximize performance in speed and problem size.

2. An efficient means of storing data arrays has been implemented in SAC. A dynamic data storage scheme eliminates the use of oversized arrays in the program routines so computer memory is not used to store unnecessary rows and columns of zeros.

3. Typically, with large finite element problems, a substantial amount of computer memory is required to store the global stiffness matrix which is generated in the execution of the analysis program. This problem has been minimized in SAC with the utilization of an efficient skyline solver. The intent of a skyline solver is to take advantage of the sparse population of relevant terms and the symmetry of the stiffness matrix. Only the nonzero terms in the upper half of the stiffness matrix are stored. Another feature employed to reduce memory requirements is a column height minimization process. This procedure enhances the efficiency of the skyline solver by optimizing the equation numbers associated with each degree of freedom. The effect is that nonzero column heights in the stiffness matrix are minimized. Therefore, no effort is required in producing meshes with efficient nodal numbering.

4. Perhaps the most significant feature of SAC implementation is the use of the Lahey EM/32 compiler and linker. This feature enables the program to use extended memory as well as virtual memory for data storage, thus memory limitations are that of the machine rather than the normal amount accessible by a DOS operating system. This compiler also takes advantage of 32-bit processing of 386 and 486 computers so that processing speed is approximately twice that of programs created with standard PC compilers. Utilization of the Lahey compiler and operating system has increased the level of PC performance to that of many workstations. The use of this compiler, however, requires that the program be run on a 386 or 486 computer with sufficient extended memory of at least 1 megabyte. SAC is extremely portable since all of the source code is written

in standard FORTRAN 77. The program can be loaded on any main frame or workstation having a FORTRAN 77 compiler with minimal effort.

APPENDIX C: ANALYSIS INPUT AND RESULT DATA

1. A strong effort was made to make SAC a user-friendly finite element program. Data are entered into SAC with the use of an input file of ASCII format. Input data are grouped into individual blocks to simplify data entry and to increase organization. The data blocks can be presented in any order and the data in each block are entered in free format. Thus, there is no need to count columns when creating or editing input data. The entire input file and a condensed result file for the John Hollis Bankhead miter gate example are listed below. These file listings illustrate the input requirements and flexibility of SAC as well as the output presentation. A detailed description of user input is presented in the SAC users manual.

---

John Hollis Bankhead lock and dam - lower miter leaf - Black Warrior River, Alabama  
 275 548 42 4 7 30 0 0  
 1 0 0 0

GRUP  
 1 2  
 29000.0 12000.0 38774.0 154.0 12.81 0.0 57.75 0.0 0.000283 (G.1-4)  
 2 2  
 29000.0 12000.0 53812.0 305.0 20.26 0.0 68.25 0.0 0.000283 (G.5-6 A)  
 3 2  
 29000.0 12000.0 41864.0 215.0 15.06 0.0 60.75 0.0 0.000283 (G.5-6 B)  
 4 2  
 29000.0 12000.0 62206.0 574.0 25.00 0.0 75.00 0.0 0.000283 (G.7-9 A)  
 5 2  
 29000.0 12000.0 41872.0 219.0 15.10 0.0 61.00 0.0 0.000283 (G.7-9 B)  
 6 2  
 29000.0 12000.0 48408.0 516.0 20.71 0.0 68.50 0.0 0.000283 (G.7-9 C)  
 7 2  
 29000.0 12000.0 69726.0 866.0 28.64 0.0 81.50 0.0 0.000283 (G.10-13 A)  
 8 2  
 29000.0 12000.0 47478.0 348.0 17.89 0.0 66.50 0.0 0.000283 (G.10-13 B)  
 9 2  
 29000.0 12000.0 55048.0 861.0 24.64 0.0 75.50 0.0 0.000283 (G.10-13 C)  
 10 2  
 29000.0 12000.0 79848.0 1145.0 39.54 0.0 90.00 0.0 0.000283 (G.14-17 A)  
 11 2  
 29000.0 12000.0 52538.0 559.0 20.39 0.0 71.75 0.0 0.000283 (G.14-17 B)  
 12 2  
 29000.0 12000.0 59986.0 1216.0 27.14 0.0 80.75 0 0 0.000283 (G.14-17 C)  
 13 2  
 29000.0 12000.0 64179.0 505.0 30.54 0.0 78.00 0.0 0.000283 (G.18 A)  
 14 2  
 29000.0 12000.0 47478.0 348.0 17.89 0.0 66.50 0.0 0.000283 (G.18 B)  
 15 2  
 29000.0 12000.0 52733.0 644.0 22.39 0.0 72.50 0.0 0.000283 (G.18 C)  
 16 2  
 29000.0 12000.0 1134.3 339.8 340.68 0.0 69.50 18.4 0.000283 (QUOIN SEAL)  
 17 2  
 29000.0 12000.0 1134.3 339.8 340.68 0.0 69.50 -18.4 0.000283 (MITER SEAL)  
 18 2  
 29000.0 12000.0 3742.0 43.0 2.04 0.0 24.50 18.4 0.000283 (QUOIN G. A)  
 19 2  
 29000.0 12000.0 3742.0 43.0 2.04 0.0 24.50 -18.4 0.000283 (MITER G. A)



101	0	1	0	1	0	0	0	G7	"	"
110	0	1	0	1	0	0	0	G6	"	"
119	0	1	0	1	0	0	0	G5	"	"
128	0	1	0	1	0	0	0	G4	"	"
137	0	1	0	1	0	0	0	G3	"	"
146	0	1	0	1	0	0	0	G2	"	"
155	0	1	0	1	0	0	0	GUDGEON PIN		
254	0	1	1	1	1	1	1	G18 MITER CONTACT		
255	0	1	1	1	1	1	1	G17 MITER CONTACT		
256	0	1	1	1	1	1	1	G16 MITER CONTACT		
257	0	1	1	1	1	1	1	G15 MITER CONTACT		
258	0	1	1	1	1	1	1	G14 MITER CONTACT		
259	0	1	1	1	1	1	1	G13 MITER CONTACT		
260	0	1	1	1	1	1	1	G12 MITER CONTACT		
261	0	1	1	1	1	1	1	G11 MITER CONTACT		
262	0	1	1	1	1	1	1	G10 MITER CONTACT		
263	0	1	1	1	1	1	1	G9 MITER CONTACT		
264	0	1	1	1	1	1	1	G8 MITER CONTACT		
265	0	1	1	1	1	1	1	G7 MITER CONTACT		
266	0	1	1	1	1	1	1	G6 MITER CONTACT		
267	0	1	1	1	1	1	1	G5 MITER CONTACT		
268	0	1	1	1	1	1	1	G4 MITER CONTACT		
269	0	1	1	1	1	1	1	G3 MITER CONTACT		
270	0	1	1	1	1	1	1	G2 MITER CONTACT		
271	0	1	1	1	1	1	1	G1 MITER CONTACT		
275	0	0	0	0	0	0	0	LAST NODE		

COORDS

1	0	0.0	0.0	0.0	G. LINE 18
2	0	21.7	0.0	7.233	
3	0	35.1	0.0	11.7	
4	1	86.5	0.0	32.0	
8	0	653.5	0.0	32.0	
9	0	704.9	0.0	11.7	
10	0	740.0	0.0	0.0	
11	0	0.0	48.0	0.0	G. LINE 17
12	0	35.1	48.0	11.7	
13	1	86.5	48.0	32.0	
17	0	653.5	48.0	32.0	
18	0	704.9	48.0	11.7	
19	0	740.0	48.0	0.0	
20	0	0.0	96.0	0.0	G. LINE 16
21	0	35.1	96.0	11.7	
22	1	86.5	96.0	32.0	
26	0	653.5	96.0	32.0	
27	0	704.9	96.0	11.7	
28	0	740.0	96.0	0.0	
29	0	0.0	144.0	0.0	G. LINE 15
30	0	35.1	144.0	11.7	
31	1	86.5	144.0	32.0	
35	0	653.5	144.0	32.0	
36	0	704.9	144.0	11.7	
37	0	740.0	144.0	0.0	
38	0	0.0	192.0	0.0	G. LINE 14
39	0	35.1	192.0	11.7	
40	1	86.5	192.0	32.0	
44	0	653.5	192.0	32.0	
45	0	704.9	192.0	11.7	
46	0	740.0	192.0	0.0	
47	0	0.0	240.0	0.0	G. LINE 13
48	0	35.1	240.0	11.7	
49	1	86.5	240.0	32.0	
53	0	653.5	240.0	32.0	
54	0	704.9	240.0	11.7	
55	0	740.0	240.0	0.0	
56	0	0.0	288.0	0.0	G. LINE 12
57	0	35.1	288.0	11.7	
58	1	86.5	288.0	32.0	
62	0	653.5	288.0	32.0	

63	0	704.9	288.0	11.7	
64	0	740.0	288.0	0.0	
65	0	0.0	341.0	0.0	G. LINE 11
66	0	35.1	341.0	11.7	
67	1	86.5	341.0	32.0	
71	0	653.5	341.0	32.0	
72	0	704.9	341.0	11.7	
73	0	740.0	341.0	0.0	
74	0	0.0	397.0	0.0	G. LINE 10
75	0	35.1	397.0	11.7	
76	1	86.5	397.0	32.0	
80	0	653.5	397.0	32.0	
81	0	704.9	397.0	11.7	
82	0	740.0	397.0	0.0	
83	0	0.0	457.0	0.0	G. LINE 9
84	0	35.1	457.0	11.7	
85	1	86.5	457.0	32.0	
89	0	653.5	457.0	32.0	
90	0	704.9	457.0	11.7	
91	0	740.0	457.0	0.0	
92	0	0.0	520.0	0.0	G. LINE 8
93	0	35.1	520.0	11.7	
94	1	86.5	520.0	32.0	
98	0	653.5	520.0	32.0	
99	0	704.9	520.0	11.7	
100	0	740.0	520.0	0.0	
101	0	0.0	586.0	0.0	G. LINE 7
102	0	35.1	586.0	11.7	
103	1	86.5	586.0	32.0	
107	0	653.5	586.0	32.0	
108	0	704.9	586.0	11.7	
109	0	740.0	586.0	0.0	
110	0	0.0	655.0	0.0	G. LINE 6
111	0	35.1	655.0	11.7	
112	1	86.5	655.0	32.0	
116	0	653.5	655.0	32.0	
117	0	704.9	655.0	11.7	
118	0	740.0	655.0	0.0	
119	0	0.0	724.0	0.0	G. LINE 5
120	0	35.1	724.0	11.7	
121	1	86.5	724.0	32.0	
125	0	653.5	724.0	32.0	
126	0	704.9	724.0	11.7	
127	0	740.0	724.0	0.0	
128	0	0.0	796.0	0.0	G. LINE 4
129	0	35.1	796.0	11.7	
130	1	86.5	796.0	32.0	
134	0	653.5	796.0	32.0	
135	0	704.9	796.0	11.7	
136	0	740.0	796.0	0.0	
137	0	0.0	868.0	0.0	G. LINE 3
138	0	35.1	868.0	11.7	
139	1	86.5	868.0	32.0	
143	0	653.5	868.0	32.0	
144	0	704.9	868.0	11.7	
145	0	740.0	868.0	0.0	
146	0	0.0	940.0	0.0	G. LINE 2
147	0	35.1	940.0	11.7	
148	1	86.5	940.0	32.0	
152	0	653.5	940.0	32.0	
153	0	704.9	940.0	11.7	
154	0	740.0	940.0	0.0	
155	0	0.0	1012.0	0.0	G. LINE 1
156	0	35.1	1012.0	11.7	
157	1	86.5	1012.0	32.0	
161	0	653.5	1012.0	32.0	
162	0	704.9	1012.0	11.7	
163	0	740.0	1012.0	0.0	
164	1	86.5	0.0	69.5	G.18 PL. PLANE

168	0	653.0	0.0	69.5	
169	1	86.5	48.0	69.5	G.17 PL. PLANE
173	0	653.0	48.0	69.5	
174	1	86.5	96.0	69.5	G.16 PL. PLANE
178	0	653.0	96.0	69.5	
179	1	86.5	144.0	69.5	G.15 PL. PLANE
183	0	653.0	144.0	69.5	
184	1	86.5	192.0	69.5	G.14 PL. PLANE
188	0	653.0	192.0	69.5	
189	1	86.5	240.0	69.5	G.13 PL. PLANE
193	0	653.0	240.0	69.5	
194	1	86.5	288.0	69.5	G.12 PL. PLANE
198	0	653.0	288.0	69.5	
199	1	86.5	341.0	69.5	G.11 PL. PLANE
203	0	653.0	341.0	69.5	
204	1	86.5	397.0	69.5	G.10 PL. PLANE
208	0	653.0	397.0	69.5	
209	1	86.5	457.0	69.5	G. 9 PL. PLANE
213	0	653.0	457.0	69.5	
214	1	86.5	520.0	69.5	G. 8 PL. PLANE
218	0	653.0	520.0	69.5	
219	1	86.5	586.0	69.5	G. 7 PL. PLANE
223	0	653.0	586.0	69.5	
224	1	86.5	655.0	69.5	G. 6 PL. PLANE
228	0	653.0	655.0	69.5	
229	1	86.5	724.0	69.5	G. 5 PL. PLANE
233	0	653.0	724.0	69.5	
234	1	86.5	796.0	69.5	G. 4 PL. PLANE
238	0	653.0	796.0	69.5	
239	1	86.5	868.0	69.5	G. 3 PL. PLANE
243	0	653.0	868.0	69.5	
244	1	86.5	940.0	69.5	G. 2 PL. PLANE
248	0	653.0	940.0	69.5	
249	1	86.5	1012.0	69.5	G. 1 PL. PLANE
253	0	653.0	1012.0	69.5	
254	0	1480.0	0.0	-246.67	G18 MITER CONTACT
255	0	1480.0	48.0	-246.67	G17 MITER CONTACT
256	0	1480.0	96.0	-246.67	G16 MITER CONTACT
257	0	1480.0	144.0	-246.67	G15 MITER CONTACT
258	0	1480.0	192.0	-246.67	G14 MITER CONTACT
259	0	1480.0	240.0	-246.67	G13 MITER CONTACT
260	0	1480.0	288.0	-246.67	G12 MITER CONTACT
261	0	1480.0	341.0	-246.67	G11 MITER CONTACT
262	0	1480.0	397.0	-246.67	G10 MITER CONTACT
263	0	1480.0	457.0	-246.67	G9 MITER CONTACT
264	0	1480.0	520.0	-246.67	G8 MITER CONTACT
265	0	1480.0	586.0	-246.67	G7 MITER CONTACT
266	0	1480.0	655.0	-246.67	G6 MITER CONTACT
267	0	1480.0	724.0	-246.67	G5 MITER CONTACT
268	0	1480.0	796.0	-246.67	G4 MITER CONTACT
269	0	1480.0	868.0	-246.67	G3 MITER CONTACT
270	0	1480.0	940.0	-246.67	G2 MITER CONTACT
271	0	1480.0	1012.0	-246.67	G1 MITER CONTACT
272	0	86.5	0.0	-6.125	N4 DIAGONAL NODE
273	0	653.5	0.0	-7.500	N8 DIAGONAL NODE
274	0	86.5	1012.0	-6.500	N157 DIAGONAL NODE
275	0	653.5	1012.0	-5.125	N161 DIAGONAL NODE

ELEM					
1	0	13	1	2	G. 18
2	0	13	2	3	
3	0	13	3	4	
4	0	14	4	5	
5	0	15	5	6	
6	0	15	6	7	
7	0	14	7	8	
8	0	13	8	9	
9	0	13	9	10	
10	0	10	11	12	G. 17

11	0	10	12	13	
12	0	11	13	14	
13	0	12	14	15	
14	0	12	15	16	
15	0	11	16	17	
16	0	10	17	18	
17	0	10	18	19	
18	0	10	20	21	G. 16
19	0	10	21	22	
20	0	11	22	23	
21	0	12	23	24	
22	0	12	24	25	
23	0	11	25	26	
24	0	10	26	27	
25	0	10	27	28	
26	0	10	29	30	G. 15
27	0	10	30	31	
28	0	11	31	32	
29	0	12	32	33	
30	0	12	33	34	
31	0	11	34	35	
32	0	10	35	36	
33	0	10	36	37	
34	0	10	38	39	G. 14
35	0	10	39	40	
36	0	11	40	41	
37	0	12	41	42	
38	0	12	42	43	
39	0	11	43	44	
40	0	10	44	45	
41	0	10	45	46	
42	0	7	47	48	G. 13
43	0	7	48	49	
44	0	8	49	50	
45	0	9	50	51	
46	0	9	51	52	
47	0	8	52	53	
48	0	7	53	54	
49	0	7	54	55	
50	0	7	56	57	G. 12
51	0	7	57	58	
52	0	8	58	59	
53	0	9	59	60	
54	0	9	60	61	
55	0	8	61	62	
56	0	7	62	63	
57	0	7	63	64	
58	0	7	65	66	G. 11
59	0	7	66	67	
60	0	8	67	68	
61	0	9	68	69	
62	0	9	69	70	
63	0	8	70	71	
64	0	7	71	72	
65	0	7	72	73	
66	0	7	74	75	G. 10
67	0	7	75	76	
68	0	8	76	77	
69	0	9	77	78	
70	0	9	78	79	
71	0	8	79	80	
72	0	7	80	81	
73	0	7	81	82	
74	0	4	83	84	G. 9
75	0	4	84	85	
76	0	5	85	86	
77	0	6	86	87	
78	0	6	87	88	
79	0	5	88	89	

80	0	4	89	90	
81	0	4	90	91	
82	0	4	92	93	G. 8
83	0	4	93	94	
84	0	5	94	95	
85	0	6	95	96	
86	0	6	96	97	
87	0	5	97	98	
88	0	4	98	99	
89	0	4	99	100	
90	0	4	101	102	G. 7
91	0	4	102	103	
92	0	5	103	104	
93	0	6	104	105	
94	0	6	105	106	
95	0	5	106	107	
96	0	4	107	108	
97	0	4	108	109	
98	0	2	110	111	G. 6
99	0	2	111	112	
100	0	3	112	113	
101	0	3	113	114	
102	0	3	114	115	
103	0	3	115	116	
104	0	2	116	117	
105	0	2	117	118	
106	0	2	119	120	G. 5
107	0	2	120	121	
108	0	3	121	122	
109	0	3	122	123	
110	0	3	123	124	
111	0	3	124	125	
112	0	2	125	126	
113	0	2	126	127	
114	0	1	128	129	G. 4
115	0	1	129	130	
116	0	1	130	131	
117	0	1	131	132	
118	0	1	132	133	
119	0	1	133	134	
120	0	1	134	135	
121	0	1	135	136	
122	0	1	137	138	G. 3
123	0	1	138	139	
124	0	1	139	140	
125	0	1	140	141	
126	0	1	141	142	
127	0	1	142	143	
128	0	1	143	144	
129	0	1	144	145	
130	0	1	146	147	G. 2
131	0	1	147	148	
132	0	1	148	149	
133	0	1	149	150	
134	0	1	150	151	
135	0	1	151	152	
136	0	1	152	153	
137	0	1	153	154	
138	0	1	155	156	G. 1
139	0	1	156	157	
140	0	1	157	158	
141	0	1	158	159	
142	0	1	159	160	
143	0	1	160	161	
144	0	1	161	162	
145	0	1	162	163	
146	0	16	1	11	Quoin seal
147	9	16	11	20	
162	0	16	146	155	

163	9	22	3	12			Quoin G. C.
175	0	22	111	120			
176	0	20	120	129			Quoin G. B.
177	9	18	129	138			Quoin G. A.
179	0	18	147	156			
180	0	25	4	13			Diaphragm 1 B
181	9	24	13	22			Diaphragm 1 A
196	0	24	148	157			
197	0	25	5	14			Diaphragm 2 B
198	9	24	14	23			Diaphragm 2 A
213	0	24	149	158			
214	0	25	6	15			Diaphragm 3 B
215	9	24	15	24			Diaphragm 3 A
230	0	24	150	159			
231	0	25	7	16			Diaphragm 4 B
232	9	24	16	25			Diaphragm 4 A
247	0	24	151	160			
248	0	25	8	17			Diaphragm 5 B
249	9	24	17	26			Diaphragm 5 A
264	0	24	152	161			
265	9	23	9	18			Miter G. C.
277	0	23	111	126			
278	0	21	126	135			Miter G. B.
279	9	19	135	144			Miter G. A.
281	0	19	153	162			
282	9	17	10	19			Miter seal
298	0	17	154	163			
299	0	38	1	3	12	11	Quoin V. Plate 17-18
300	0	38	3	4	13	12	
301	1	31	164	165	170	169	Skin Plate 17-18
304	0	31	167	168	173	172	
305	0	38	8	9	18	17	Miter V. Plate 17-18
306	0	38	9	10	19	18	
307	0	38	11	12	21	20	Quoin V. Plate 16-17
308	0	38	12	13	22	21	
309	1	31	169	170	175	174	Skin Plate 16-17
312	0	31	172	173	178	177	
313	0	38	17	18	27	26	Miter V. Plate 16-17
314	0	38	18	19	28	27	
315	0	38	20	21	30	29	Quoin V. Plate 15-16
316	0	38	21	22	31	30	
317	1	31	174	175	180	179	Skin Plate 15-16
320	0	31	177	178	183	182	
321	0	38	26	27	36	35	Miter V. Plate 15-16
322	0	38	27	28	37	36	
323	0	38	29	30	39	38	Quoin V. Plate 14-15
324	0	38	30	31	40	39	
325	1	31	179	180	185	184	Skin Plate 14-15
328	0	31	182	183	188	187	
329	0	38	35	36	45	44	Miter V. Plate 14-15
330	0	38	36	37	46	45	
331	0	37	38	39	48	47	Quoin V. Plate 13-14
332	0	37	39	40	49	48	
333	1	30	184	185	190	189	Skin Plate 13-14
336	0	30	187	188	193	192	
337	0	37	44	45	54	53	Miter V. Plate 13-14
338	0	37	45	46	55	54	
339	0	36	47	48	57	56	Quoin V. Plate 12-13
340	0	36	48	49	58	57	
341	1	30	189	190	195	194	Skin Plate 12-13
344	0	30	192	193	198	197	
345	0	36	53	54	63	62	Miter V. Plate 12-13
346	0	36	54	55	64	63	
347	0	36	56	57	66	65	Quoin V. Plate 11-12
348	0	36	57	58	67	66	
349	1	30	194	195	200	199	Skin Plate 11-12
352	0	30	197	198	203	202	
353	0	36	62	63	72	71	Miter V. Plate 11-12
354	0	36	63	64	73	72	

355	0	36	65	66	75	74	Quoin V. Plate 10-11
356	0	36	66	67	76	75	Skin Plate 10-11
357	1	30	199	200	205	204	Miter V. Plate 10-11
360	0	30	202	203	208	207	Quoin V. Plate 9-10
361	0	36	71	72	81	80	Skin Plate 9-10
362	0	36	72	73	82	81	Miter V. Plate 9-10
363	0	36	74	75	84	83	Quoin V. Plate 8-9
364	0	36	75	76	85	84	Skin Plate 8-9
365	1	30	204	205	210	209	Miter V. Plate 8-9
368	0	30	207	208	213	212	Quoin V. Plate 7-8
369	0	36	80	81	90	89	Skin Plate 7-8
370	0	36	81	82	91	90	Miter V. Plate 7-8
371	0	35	83	84	93	92	Quoin V. Plate 6-7
372	0	35	84	85	94	93	Skin Plate 6-7
373	1	29	209	210	215	214	Miter V. Plate 6-7
376	0	29	212	213	218	217	Quoin V. Plate 5-6
377	0	35	89	90	99	98	Skin Plate 5-6
378	0	35	90	91	100	99	Miter V. Plate 5-6
379	0	35	92	93	102	101	Quoin V. Plate 4-5
380	0	35	93	94	103	102	Skin Plate 4-5
381	1	28	214	215	220	219	Miter V. Plate 4-5
384	0	28	217	218	223	222	Quoin V. Plate 3-4
385	0	35	98	99	108	107	Skin Plate 3-4
386	0	35	99	100	109	108	Miter V. Plate 3-4
387	0	35	101	102	111	110	Quoin V. Plate 2-3
388	0	35	102	103	112	111	Skin Plate 2-3
389	1	28	219	220	225	224	Miter V. Plate 2-3
392	0	28	222	223	228	227	Quoin V. Plate 1-2
393	0	35	107	108	117	116	Skin Plate 1-2
394	0	35	108	109	118	117	Miter V. Plate 1-2
395	0	34	110	111	120	119	Quoin V. Plate 1-2
396	0	34	111	112	121	120	Skin Plate 1-2
397	1	27	224	225	230	229	Miter V. Plate 1-2
400	0	27	227	228	233	232	Quoin V. Plate 1-2
401	0	34	116	117	126	125	Skin Plate 1-2
402	0	34	117	118	127	126	Miter V. Plate 1-2
403	0	33	119	120	129	128	Quoin V. Plate 1-2
404	0	33	120	121	130	129	Skin Plate 1-2
405	1	26	229	230	235	234	Miter V. Plate 1-2
408	0	26	232	233	238	237	Quoin V. Plate 1-2
409	0	33	125	126	135	134	Skin Plate 1-2
410	0	33	126	127	136	135	Miter V. Plate 1-2
411	0	32	128	129	138	137	Quoin V. Plate 1-2
412	0	32	129	130	139	138	Skin Plate 1-2
413	1	26	234	235	240	239	Miter V. Plate 1-2
416	0	26	237	238	243	242	Quoin V. Plate 1-2
417	0	32	134	135	144	143	Skin Plate 1-2
418	0	32	135	136	145	144	Miter V. Plate 1-2
419	0	32	137	138	147	146	Quoin V. Plate 1-2
420	0	32	138	139	148	147	Skin Plate 1-2
421	1	26	239	240	245	244	Miter V. Plate 1-2
424	0	26	242	243	248	247	Quoin V. Plate 1-2
425	0	32	143	144	153	152	Skin Plate 1-2
426	0	32	144	145	154	153	Miter V. Plate 1-2
427	0	32	146	147	156	155	Quoin V. Plate 1-2
428	0	32	147	148	157	156	Skin Plate 1-2
429	1	26	244	245	250	249	Miter V. Plate 1-2
432	0	26	247	248	253	252	Quoin V. Plate 1-2
433	0	32	152	153	162	161	Skin Plate 1-2
434	0	32	153	154	163	162	Miter V. Plate 1-2
435	1	39	4	164			Quoin V. Plate 1-2
439	0	39	8	168			Skin Plate 1-2
440	1	39	13	169			Miter V. Plate 1-2
444	0	39	17	173			Quoin V. Plate 1-2
445	1	39	22	174			Skin Plate 1-2
449	0	39	26	178			Miter V. Plate 1-2
450	1	39	31	179			Quoin V. Plate 1-2
454	0	39	35	183			Skin Plate 1-2
455	1	39	40	184			Miter V. Plate 1-2

Rigid Links to Plates

459	0	39	44	188
460	1	39	49	189
464	0	39	53	193
465	1	39	58	194
469	0	39	62	198
470	1	39	67	199
474	0	39	71	203
475	1	39	76	204
479	0	39	80	208
480	1	39	85	209
484	0	39	89	213
485	1	39	94	214
489	0	39	98	218
490	1	39	103	219
494	0	39	107	223
495	1	39	112	224
499	0	39	116	228
500	1	39	121	229
504	0	39	125	233
505	1	39	130	234
509	0	39	134	238
510	1	39	139	239
514	0	39	143	243
515	1	39	148	244
519	0	39	152	248
520	1	39	157	249
524	0	39	161	253
525	0	40	10	254
526	0	40	19	255
527	0	40	28	256
528	0	40	37	257
529	0	40	46	258
530	0	40	55	259
531	0	40	64	260
532	0	40	73	261
533	0	40	82	262
534	0	40	91	263
535	0	40	100	264
536	0	40	109	265
537	0	40	118	266
538	0	40	127	267
539	0	40	136	268
540	0	40	145	269
541	0	40	154	270
542	0	40	163	271
543	0	41	272	275
544	0	42	273	274
545	0	39	4	272
546	0	39	8	273
547	0	39	157	274
548	0	39	161	275

MITER INCLINED SUPPORT ELEMENTS

DIAGONAL N4-N161  
 DIAGONAL N8-N157  
 RIGID LINK TO DIAGONAL  
 RIGID LINK TO DIAGONAL  
 RIGID LINK TO DIAGONAL  
 RIGID LINK TO DIAGONAL

OUTB (SETUP 1: CHAN 1-10,13-32)

54	42.0	26.5	G12 : USF - MS
54	42.0	-46.2	G12 : DSF - MS
70	42.0	26.5	G10 : USF - MS
70	42.0	-46.2	G10 : DSF - MS
86	42.0	27.1	G 8 : USF - MS
86	42.0	-45.4	G 8 : DSF - MS
94	42.0	27.1	G 7 : USF - MS
94	42.0	-45.4	G 7 : DSF - MS
94	42.0	-8.4	G 7 : STIFFENER - MS
94	42.0	-45.4	G 7 : DSF - MS
544	580.0	0.0	X-BRACE 2
544	580.0	0.0	X-BRACE 2
543	580.0	0.0	X-BRACE 1
543	580.0	0.0	X-BRACE 1
110	42.0	30.5	G 5 : USF - MS
110	42.0	-42.0	G 5 : DSF - MS

226	45.0	33.2	D5-6: USF - MS
226	45.0	-39.3	D5-6: DSF - MS
126	42.0	32.1	G 3 : USF - MS
126	42.0	-40.4	G 3 : DSF - MS
142	42.0	33.6	G 1 : USF - MS
142	42.0	-40.0	G 1 : DSF - MS
87	99.8	38.5	G 8 : USF - MITER END
87	99.8	-34.8	G 8 : DSF - MITER END
95	99.8	38.5	G 7 : USF - MITER END
95	99.8	-34.8	G 7 : DSF - MITER END
84	42.0	38.5	G 8 : USF - QUOIN END
84	42.0	-34.8	G 8 : DSF - QUOIN END
92	42.0	38.5	G 7 : USF - QUOIN END
92	42.0	-34.8	G 7 : DSF - QUOIN END

```

LOAD
CASE 1      POOL LEVEL @ LIFT LINE 2 - CLICK 1
WATER LOAD
0.0      229.6    157.6  3.611e-05  2
ENDCASE 1
CASE 2      POOL LEVEL @ LIFT LINE 4 - CLICK 3
WATER LOAD
0.0      349.2    157.6  3.611e-05  2
ENDCASE 2
CASE 3      POOL LEVEL @ LIFT LINE 6 - CLICK 5
WATER LOAD
0.0      469.2    157.6  3.611e-05  2
ENDCASE 3
CASE 4      POOL LEVEL @ LIFT LINE 8 - CLICK 7
WATER LOAD
0.0      589.2    157.6  3.611e-05  2
ENDCASE 4
CASE 5      POOL LEVEL @ LIFT LINE 10 - CLICK 9
WATER LOAD
0.0      709.2    157.6  3.611e-05  2
ENDCASE 5
CASE 6      POOL LEVEL @ LIFT LINE 12 - CLICK 11
WATER LOAD
0.0      829.2    157.6  3.611e-05  2
ENDCASE 6
CASE 7      POOL LEVEL @ LIFT LINE 14 - CLICK 13
WATER LOAD
0.0      949.2    157.6  3.611e-05  2
ENDCASE 7

#CASE 1 DEAD LOAD - UNMITERED POSITION
GRAVITY LOAD
-1.0  2
ENDCASE 1

```

---

Listing of condensed result file:

=====

MICRO FINITE ELEMENT PROGRAM - SAC	PAGE 1
John Hollis Bankhead lock and dam - lower miter leaf - Black Warrior River, Alab	

=====

\*INPUT CONTROL PARAMETERS:

NUMBER OF NODAL POINTS . . . . .	253
NUMBER OF ELEMENTS . . . . .	524
NUMBER OF MATERIAL GROUPS . . . . .	39
SPATIAL DIMENSIONS . . . . .	3
MAX DEGREES OF FREEDOM/NODE . . . . .	6
MAX NUMBER OF NODES/ELEMENT . . . . .	4
NUMBER OF LOAD CASES. . . . .	1
NUMBER OF BEAMS FOR OUTPUT. . . . .	0
NUMBER OF PLATES FOR OUTPUT . . . . .	0
NUMBER OF PARAMETERS FOR OPTIMIZATION . . . . .	0

\*MATERIAL PROPERTIES

MATERIAL GROUP . . . . . 1

2-NODE EULER-BERNOULLI BEAM

ELASTIC MODULUS (E) . . . . .	2.900E+04
SHEAR MODULUS (G) . . . . .	1.200E+04
MOMENT OF INERTIA ABOUT y . . . . .	3.877E+04
MOMENT OF INERTIA ABOUT z . . . . .	5.000E+03
TORSIONAL SHAPE FACTOR (J). . . . .	1.281E+01
WARPING TORSION CONST. (Cw) . . . . .	1.853E+05
CROSS-SECTIONAL AREA. . . . .	5.775E+01
ROTATION ABOUT BEAM AXES. . . . .	0.000E+00
MATERIAL UNIT WEIGHT. . . . .	2.830E-04

MATERIAL GROUP . . . . . 2

2-NODE EULER-BERNOULLI BEAM

ELASTIC MODULUS (E) . . . . .	2.900E+04
SHEAR MODULUS (G) . . . . .	1.200E+04
MOMENT OF INERTIA ABOUT y . . . . .	5.381E+04
MOMENT OF INERTIA ABOUT z . . . . .	5.000E+03
TORSIONAL SHAPE FACTOR (J). . . . .	2.026E+01
WARPING TORSION CONST. (Cw) . . . . .	3.879E+05
CROSS-SECTIONAL AREA. . . . .	6.825E+01
ROTATION ABOUT BEAM AXES. . . . .	0.000E+00
MATERIAL UNIT WEIGHT. . . . .	2.830E-04

MATERIAL GROUP . . . . . 26

4-NODE RECTANGULAR KIRCHOFF PLATE

ELASTIC MODULUS . . . . .	1.000E-03
POISSON RATIO . . . . .	1.500E-01
ELEMENT THICKNESS . . . . .	3.750E-01
MATERIAL UNIT WEIGHT. . . . .	2.830E-04

\*NODAL COORDINATES

NODE	X-COORD	Y-COORD	Z-COORD
1	0.00000E+00	0.00000E+00	0.00000E+00
2	2.17000E+01	0.00000E+00	7.23300E+00
3	3.51000E+01	0.00000E+00	1.17000E+01
4	8.65000E+01	0.00000E+00	3.20000E+01
5	2.28250E+02	0.00000E+00	3.20000E+01
6	3.70000E+02	0.00000E+00	3.20000E+01
7	5.11750E+02	0.00000E+00	3.20000E+01
8	6.53500E+02	0.00000E+00	3.20000E+01
9	7.04900E+02	0.00000E+00	1.17000E+01
10	7.40000E+02	0.00000E+00	0.00000E+00
11	0.00000E+00	4.80000E+01	0.00000E+00
12	3.51000E+01	4.80000E+01	1.17000E+01
13	8.65000E+01	4.80000E+01	3.20000E+01
14	2.28250E+02	4.80000E+01	3.20000E+01
15	3.70000E+02	4.80000E+01	3.20000E+01
16	5.11750E+02	4.80000E+01	3.20000E+01
17	6.53500E+02	4.80000E+01	3.20000E+01
18	7.04900E+02	4.80000E+01	1.17000E+01
19	7.40000E+02	4.80000E+01	0.00000E+00
20	0.00000E+00	9.60000E+01	0.00000E+00
21	3.51000E+01	9.60000E+01	1.17000E+01
22	8.65000E+01	9.60000E+01	3.20000E+01
23	2.28250E+02	9.60000E+01	3.20000E+01
24	3.70000E+02	9.60000E+01	3.20000E+01
25	5.11750E+02	9.60000E+01	3.20000E+01
26	6.53500E+02	9.60000E+01	3.20000E+01
27	7.04900E+02	9.60000E+01	1.17000E+01
28	7.40000E+02	9.60000E+01	0.00000E+00
29	0.00000E+00	1.44000E+02	0.00000E+00
30	3.51000E+01	1.44000E+02	1.17000E+01
31	8.65000E+01	1.44000E+02	3.20000E+01
32	2.28250E+02	1.44000E+02	3.20000E+01
33	3.70000E+02	1.44000E+02	3.20000E+01
34	5.11750E+02	1.44000E+02	3.20000E+01
35	6.53500E+02	1.44000E+02	3.20000E+01
36	7.04900E+02	1.44000E+02	1.17000E+01
37	7.40000E+02	1.44000E+02	0.00000E+00
38	0.00000E+00	1.92000E+02	0.00000E+00
39	3.51000E+01	1.92000E+02	1.17000E+01
40	8.65000E+01	1.92000E+02	3.20000E+01
41	2.28250E+02	1.92000E+02	3.20000E+01
42	3.70000E+02	1.92000E+02	3.20000E+01
43	5.11750E+02	1.92000E+02	3.20000E+01
44	6.53500E+02	1.92000E+02	3.20000E+01
45	7.04900E+02	1.92000E+02	1.17000E+01
46	7.40000E+02	1.92000E+02	0.00000E+00
47	0.00000E+00	2.40000E+02	0.00000E+00

\*ELEMENT TOPOLOGY

ELEMENT	MATERIAL	1 ND	2 ND	3 ND	4 ND
1	13	1	2		
2	13	2	3		
3	13	3	4		
4	14	4	5		
5	15	5	6		
6	15	6	7		
7	14	7	8		
8	13	8	9		
9	13	9	10		
10	10	11	12		
11	10	12	13		
12	11	13	14		
13	12	14	15		
14	12	15	16		
15	11	16	17		
16	10	17	18		
17	10	18	19		
18	10	20	21		
19	10	21	22		
20	11	22	23		
299	38	1	3	12	11
300	38	3	4	13	12
301	31	164	165	170	169
302	31	165	166	171	170
303	31	166	167	172	171
304	31	167	168	173	172
305	38	8	9	18	17
306	38	9	10	19	18
307	38	11	12	21	20
308	38	12	13	22	21
309	31	169	170	175	174
310	31	170	171	176	175
311	31	171	172	177	176
312	31	172	173	178	177
313	38	17	18	27	26
314	38	18	19	28	27
315	38	20	21	30	29
316	38	21	22	31	30
317	31	174	175	180	179
318	31	175	176	181	180
319	31	176	177	182	181
320	31	177	178	183	182
321	38	26	27	36	35
322	38	27	28	37	36
323	38	29	30	39	38
324	38	30	31	40	39
325	31	179	180	185	184
326	31	180	181	186	185
327	31	181	182	187	186
328	31	182	183	188	187
329	38	35	36	45	44
330	38	36	37	46	45
331	37	38	39	48	47
332	37	39	40	49	48

\*NODAL RESTRAINT CONDITIONS

NODE	X-DISP	Y-DISP	Z-DISP	X-ROT	Y-ROT	Z-ROT
2	1	1	1	0	0	0
7	0	0	1	0	0	0
155	1	0	1	1	0	1

\*SKYLINE OPTIMIZATION RESULTS

INITIAL VALUES:  
 MAXIMUM COLUMN HEIGHT: 961  
 SIZE OF GLOBAL STIFFNESS VECTOR: 3708.432 KB  
 OPTIMIZED VALUES:  
 MAXIMUM COLUMN HEIGHT: 143  
 SIZE OF GLOBAL STIFFNESS VECTOR: 1098.904 KB

\*\*\*\*\*  
 \*\*\*\*\* LOAD DATA FOR LOAD CASE # 1 \*\*\*\*\*  
 \*\*\*\*\*

\*APPLIED GRAVITY LOADS

GRAVITY FACTOR . . . . . -1.00  
 GRAVITY DIRECTION CODE . . . . . 2

\*\*\*\*\*  
 \*\*\*\*\* OUTPUT FOR LOAD CASE # 1 \*\*\*\*\*  
 \*\*\*\*\*

\*NODAL DISPLACEMENTS IN GLOBAL COORDINATES

NODE	X-DISP	Y-DISP	Z-DISP	X-ROT	Y-ROT	Z-ROT
1	0.1050E-02	-.3308E-02	-.2263E-02	-.2430E-03	-.1068E-03	0.1298E-03
2	0.0000E+00	0.0000E+00	0.0000E+00	-.1843E-03	-.1112E-03	-.1278E-03
3	-.1774E-02	-.3069E-02	0.1096E-02	-.1139E-03	-.1151E-03	-.3582E-03
4	-.7381E-02	-.2925E-01	0.5657E-02	-.5105E-03	-.1058E-03	-.6095E-03
5	-.1202E-01	-.1333E+00	0.1405E-01	-.1447E-02	-.1427E-04	-.5573E-03
6	-.1317E-01	-.2178E+00	0.1128E-01	-.2273E-02	0.5214E-04	-.4978E-03
7	-.1300E-01	-.2888E+00	0.0000E+00	-.3047E-02	0.1069E-03	-.4445E-03
8	-.1242E-01	-.3486E+00	-.2030E-01	-.3763E-02	0.1897E-03	-.4013E-03
9	-.1640E-01	-.4453E+00	-.3077E-01	-.3983E-02	0.2133E-03	-.3055E-03
10	-.1893E-01	-.5022E+00	-.3839E-01	-.4063E-02	0.2190E-03	-.2584E-03
11	0.4811E-02	-.9313E-02	0.5650E-03	-.5145E-04	0.2312E-03	-.1316E-03
12	0.7995E-02	-.1395E-01	-.7392E-02	-.1712E-03	0.2312E-03	-.2232E-03
13	0.1251E-01	-.3020E-01	-.1942E-01	-.5272E-03	0.2350E-03	-.4345E-03
14	0.9933E-02	-.1334E+00	-.5542E-01	-.1447E-02	0.2767E-03	-.4794E-03
15	0.8387E-02	-.2178E+00	-.9784E-01	-.2274E-02	0.3211E-03	-.4524E-03
16	0.7540E-02	-.2887E+00	-.1463E+00	-.3049E-02	0.3621E-03	-.4257E-03
17	0.7086E-02	-.3486E+00	-.2009E+00	-.3767E-02	0.4090E-03	-.3969E-03
18	-.1376E-02	-.4453E+00	-.2222E+00	-.3999E-02	0.4172E-03	-.3037E-03
19	-.6292E-02	-.5021E+00	-.2368E+00	-.4073E-02	0.4187E-03	-.2467E-03
20	0.1174E-01	-.1551E-01	0.1285E-02	-.1204E-03	0.5454E-03	-.1520E-03
21	0.1814E-01	-.2087E-01	-.1786E-01	-.2279E-03	0.5458E-03	-.2512E-03
22	0.2925E-01	-.3329E-01	-.4596E-01	-.5676E-03	0.5482E-03	-.4087E-03
23	0.2832E-01	-.1337E+00	-.1249E+00	-.1450E-02	0.5677E-03	-.4410E-03

\*INTERNAL FORCES FOR BEAMS

ELEMENT	NODE	AXIAL	SHEAR-Y	SHEAR-Z	TORSION	MOMENT-Y	MOMENT-Z
1	1	27.70	-253.05	26.36	437.83	50.07	-1226.97
	2	-27.70	253.05	-26.36	-437.83	-653.06	-4561.11
2	2	213.98	295.73	-18.26	438.00	653.06	4561.10
	3	-213.98	-295.73	18.26	-438.00	-395.11	-383.94
3	3	144.88	78.87	-26.19	557.89	408.61	2410.28
	4	-144.88	-78.87	26.19	-557.89	1038.86	1948.19
4	4	63.12	13.05	0.66	43.49	-935.71	871.70
	5	-63.12	-13.05	-0.66	-43.49	841.88	978.66
5	5	17.07	5.96	0.53	61.53	-753.79	361.70
	6	-17.07	-5.96	-0.53	-61.53	679.00	483.43
6	6	-2.51	2.52	0.10	57.65	-597.58	123.87
	7	2.51	-2.52	-0.10	-57.65	583.40	232.86
7	7	-7.90	-0.04	-4.22	33.23	-506.13	-46.68
	8	7.90	0.04	4.22	-33.23	1103.65	41.69
8	8	-6.02	-1.34	8.78	291.04	-1037.27	-57.91
	9	6.02	1.34	-8.78	-291.04	551.94	-15.97
9	9	-0.39	-2.92	13.90	362.92	-543.99	-130.62
	10	0.39	2.92	-13.90	-362.92	29.57	22.76
10	11	-35.61	-9.72	0.24	1359.01	-3.54	12.28
	12	35.61	9.72	-0.24	-1359.01	-5.19	-371.86
11	12	10.25	66.28	-5.81	1170.72	3.95	2003.93
	13	-10.25	-66.28	5.81	-1170.72	317.17	1658.89
12	13	37.85	23.45	-1.74	66.81	-326.07	1708.07
	14	-37.85	-23.45	1.74	-66.81	572.09	1616.15
13	14	25.55	11.26	0.40	106.95	-572.65	770.54
	15	-25.55	-11.26	-0.40	-106.95	516.34	825.89
14	15	13.99	5.29	0.18	100.27	-516.31	347.49
	16	-13.99	-5.29	-0.18	-100.27	490.50	402.06
15	16	6.68	0.97	-0.18	52.18	-490.94	38.96
	17	-6.68	-0.97	0.18	-52.18	516.63	97.92
16	17	3.14	-1.61	6.11	716.75	-513.66	-48.16
	18	-3.14	1.61	-6.11	-716.75	176.19	-40.75
17	18	1.72	-3.04	4.64	838.37	-175.36	-176.82
	19	-1.72	3.04	-4.64	-838.37	3.65	64.17
18	20	-1.52	11.14	-1.22	1269.92	-2.86	441.55
	21	1.52	-11.14	1.22	-1269.92	48.13	-29.40
19	21	-0.34	36.46	-1.86	1071.04	-48.90	1064.53
	22	0.34	-36.46	1.86	-1071.04	151.71	950.61
20	22	13.69	24.52	-0.73	64.08	-157.27	1771.13
	23	-13.69	-24.52	0.73	-64.08	260.74	1704.92
21	23	15.37	14.06	-0.49	106.90	-262.18	976.85
	24	-15.37	-14.06	0.49	-106.90	331.20	1016.46
22	24	11.93	7.48	0.22	100.83	-330.74	513.03
	25	-11.93	-7.48	-0.22	-100.83	299.30	547.79
23	25	7.70	2.31	0.88	53.07	-298.63	144.92
	26	-7.70	-2.31	-0.88	-53.07	174.42	182.43
24	26	3.92	0.28	1.86	780.20	-170.77	6.52
	27	-3.92	-0.28	-1.86	-780.20	67.71	8.84
25	27	1.60	-1.29	1.75	934.70	-67.11	-152.63
	28	-1.60	1.29	-1.75	-934.70	2.36	105.00
26	29	0.13	15.38	-1.31	1218.83	-2.06	482.34
	30	-0.13	-15.38	1.31	-1218.83	50.69	86.55
27	30	2.95	25.72	-1.54	1011.51	-51.22	773.17
	31	-2.95	-25.72	1.54	-1011.51	136.23	647.96
28	31	7.24	23.53	0.33	61.82	-139.97	1693.63
	32	-7.24	-23.53	-0.33	-61.82	93.18	1641.61

\*SUMMATION OF APPLIED FORCES

F(X)	F(Y)	F(Z)	M(X)	M(Y)	M(Z)
0.000E+00	-5.492E+02	0.000E+00	0.000E+00	0.000E+00	0.000E+00

\*NODAL REACTIONS AT FIXED NODES

NODE #	F(X)	F(Y)	F(Z)	M(X)	M(Y)	M(Z)
2	190.831	549.183	16.579	0.000	0.000	0.000
7	0.000	0.000	-4.315	0.000	0.000	0.000
155	-190.831	0.000	-12.264	-609.411	0.000	-2203.841

\*SUMMATION OF APPLIED FORCES AND REACTIONS

F(X)	F(Y)	F(Z)	M(X)	M(Y)	M(Z)
-4.369E-06	-5.511E-07	-2.448E-04	-6.094E-08	0.000E+00	-2.204E-06

TOTAL RUN TIME (HH:MM:SS.hh) = 00:02:55.98

## APPENDIX D: A DEVELOPMENT OF WARPING TORSION TERMS

1. Restraint of torsional flange warping can be represented in two ways. One method is to use a three-dimensional modeling approach in which the member flanges are modeled independently. This approach results in independent displacements of each flange rather than having only a single set of displacements for a given girder or diaphragm cross section. The other approach is to implement restrained warping torsion terms into the torsional stiffness of the frame elements. The development of warping torsion stiffness terms is available in most advanced steel design and structural analysis references. However, warping constants are not often incorporated in ordinary frame analysis since the connection details of most structures do not warrant consideration of warping torsion, and its effect is generally not significant to overall frame behavior. Following is a brief development of the warping torsion terms that may be applied in the element stiffness matrices for the examples which consider warping torsion.

2. The total torsional resistance of a given I-shaped cross section is the summation of St. Venant's torsion and the restrained flange warping torsion.

$$T = T_1 + T_2 \quad (D1)$$

where  $T_1$  is St. Venant's torsion and  $T_2$  is the restrained warping torsion. The expression for St. Venant's torsion is

$$T_1 = \frac{GJ\theta}{L} \quad (D2)$$

where  $G$  is the shear modulus,  $J$  the polar moment of inertia,  $\theta$  the angle of twist, and  $L$  the torsional unbraced length.

3. The warping torsion terms are due to the bending resistance of the flanges about their strong axes. The forces that are generated when the flanges are braced against warping are illustrated in Figure D1. Applying basic beam theory to obtain the resistance of a single flange yields

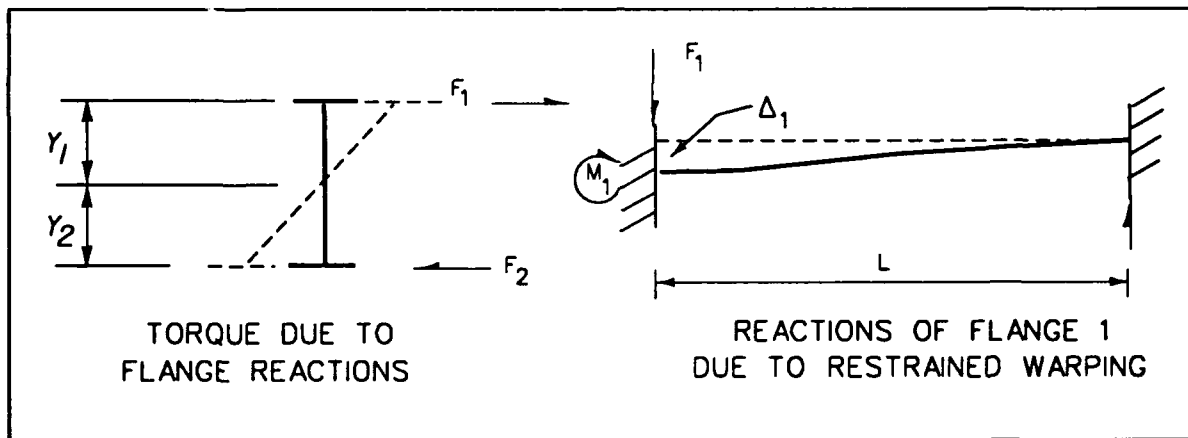


Figure D1. Restrainted warping torsion in beam flanges

$$F_f = \frac{12EI_f \Delta_f}{L^3} \quad \text{and} \quad M_f = \frac{6EI_f \Delta_f}{L^2} \quad (\text{D3})$$

where the subscript f designates flange,  $I_f$  is the flange moment of inertia about its strong axis,  $F_f$  and  $M_f$  represent the flange force and moment resultants due to a displacement  $\Delta$ , and  $L$  is the torsional unbraced length. The torque applied by the warping torsion  $T_2$  is then the summation of the flange forces  $F_1$  times their respective distances to the neutral axis  $y_1$ .

$$T_2 = \sum F_1(y_1) = F_1(y_1) + F_2(y_2) \quad (\text{D4})$$

Substitution of the expression for  $F_f$  of Equation D3 into Equation D4 yields

$$T_2 = \sum_1 \frac{12 E I_1 \Delta_1 y_1}{L^3} \quad (D5)$$

For an angle of twist  $\theta$  assuming small displacement theory

$$\theta \approx \tan \theta = \frac{\Delta_1}{y_1} \quad (D6)$$

Therefore,

$$\Delta_1 \approx y_1 \theta \quad (D7)$$

Substituting the expression for  $\Delta_1$  into Equation D5 yields

$$T_2 = \frac{12 E \theta}{L^3} \sum I_1 y_1^2 \quad (D8)$$

The summation terms in Equation D8 are known as the warping constant of a cross section  $C_w$ .

$$C_w = \sum I_1 y_1^2 \quad (D9)$$

4. For symmetric I sections it is assumed that the moment of inertia about the weak axis  $I_y$  is due only to the flanges, simplifying the calculation of the warping constant as

$$C_w = \frac{I_y d^2}{4} \quad (D10)$$

where  $d$  is the depth of the I section. Substituting Equations D2, D8 and D9 into Equation D1 yields the magnitude of the overall torsional resistance  $T$ .

$$T = \frac{G J \theta}{L} + \frac{12 E C_w \theta}{L^3} \quad (D11)$$

### **Waterways Experiment Station Cataloging-in-Publication Data**

Computer-aided, field-verified structural evaluation. Report 1, Development of computer modeling techniques for miter lock gates / by Brett C. Commander ... [et al.] ; prepared for Department of the Army, US Army Corps of Engineers.

62 p. : ill. ; 28 cm. — (Technical report ; ITL-92-12)

Includes bibliographical references.

1. Hydraulic gates — Computer simulation. 2. Locks (Hydraulic engineering) — Evaluation — Data processing. 3. Structural analysis (Engineering) — Data processing. I. Commander, Brett C. II. United States Army. Corps of Engineers. III. US Army Engineer Waterways Experiment Station. IV. Computer-aided Structural Engineering Project. V. Title: Development of computer modeling techniques for miter lock gates. VI. Series: Technical report (US Army Engineer Waterways Experiment Station) ; ITL-92-12.

TA7 W34 no.ITL-92-12

**WATERWAYS EXPERIMENT STATION REPORTS  
PUBLISHED UNDER THE COMPUTER-AIDED  
STRUCTURAL ENGINEERING (CASE) PROJECT**

	Title	Date
Technical Report K-78-1	List of Computer Programs for Computer Aided Structural Engineering	Feb 1979
Instruction Report O-79-2	User's Guide: Computer Program with interactive Graphics for Analysis of Plané Frame Structures (CFRAME)	Mar 1979
Technical Report K-80-1	Survey of Bridge-Oriented Design Software	Jan 1980
Technical Report K-80-2	Evaluation of Computer Programs for the Design/Analysis of Highway and Railway Bridges	Jan 1980
Instruction Report K-80-1	User's Guide: Computer Program for Design Review of Curvilinear Conduits/Culverts (CURCON)	Feb 1980
Instruction Report K-80-3	A Three-Dimensional Finite Element Data Edit Program	Mar 1980
Instruction Report K-80-4	A Three-Dimensional Stability Analysis/Design Program (3DSAD) Report 1: General Geometry Module Report 3: General Analysis Module (CGAM) Report 4: Special-Purpose Modules for Dams (CDAMS)	Jun 1980 Jun 1982 Aug 1983
Instruction Report K-80-6	Basic User's Guide: Computer Program for Design and Analysis of Inverted-T Retaining Walls and Floodwalls (TWDA)	Dec 1980
Instruction Report K-80-7	User's Reference Manual: Computer Program for Design and Analysis of Inverted-T Retaining Walls and Floodwalls (TWDA)	Dec 1980
Technical Report K-80-4	Documentation of Finite Element Analyses Report 1: Longview Outlet Works Conduit Report 2: Anchored Wall Monolith, Bay Springs Lock	Dec 1980 Dec 1980
Technical Report K-80-5	Basic Pile Group Behavior	Dec 1980
Instruction Report K-81-2	User's Guide: Computer Program for Design and Analysis of Sheet Pile Walls by Classical Methods (CSHTWAL) Report 1: Computational Processes Report 2: Interactive Graphics Options	Feb 1981 Mar 1981
Instruction Report K-81-3	Validation Report: Computer Program for Design and Analysis of Inverted-T Retaining Walls and Floodwalls (TWDA)	Feb 1981
Instruction Report K-81-4	User's Guide: Computer Program for Design and Analysis of Cast-in-Place Tunnel Linings (NEWTUN)	Mar 1981
Instruction Report K-81-6	User's Guide: Computer Program for Optimum Nonlinear Dynamic Design of Reinforced Concrete Slabs Under Blast Loading (CBARCS)	Mar 1981
Instruction Report K-81-7	User's Guide: Computer Program for Design or Investigation of Orthogonal Culverts (CORTCUL)	Mar 1981
Instruction Report K-81-9	User's Guide: Computer Program for Three-Dimensional Analysis of Building Systems (CTABS80)	Aug 1981
Technical Report K-81-2	Theoretical Basis for CTABS80: A Computer Program for Three-Dimensional Analysis of Building Systems	Sep 1981
Instruction Report K-82-6	User's Guide: Computer Program for Analysis of Beam-Column Structures with Nonlinear Supports (CBEAMC)	Jun 1982

(Continued)

**WATERWAYS EXPERIMENT STATION REPORTS  
PUBLISHED UNDER THE COMPUTER-AIDED  
STRUCTURAL ENGINEERING (CASE) PROJECT**

(Continued)

	Title	Date
Instruction Report K-82-7	User's Guide: Computer Program for Bearing Capacity Analysis of Shallow Foundations (CBEAR)	Jun 1982
Instruction Report K-83-1	User's Guide: Computer Program with Interactive Graphics for Analysis of Plane Frame Structures (CFRAME)	Jan 1983
Instruction Report K-83-2	User's Guide: Computer Program for Generation of Engineering Geometry (SKETCH)	Jun 1983
Instruction Report K-83-5	User's Guide: Computer Program to Calculate Shear, Moment, and Thrust (CSMT) from Stress Results of a Two-Dimensional Finite Element Analysis	Jul 1983
Technical Report K-83-1	Basic Pile Group Behavior	Sep 1983
Technical Report K-83-3	Reference Manual: Computer Graphics Program for Generation of Engineering Geometry (SKETCH)	Sep 1983
Technical Report K-83-4	Case Study of Six Major General-Purpose Finite Element Programs	Oct 1983
Instruction Report K-84-2	User's Guide: Computer Program for Optimum Dynamic Design of Nonlinear Metal Plates Under Blast Loading (CSDOOR)	Jan 1984
Instruction Report K-84-7	User's Guide: Computer Program for Determining Induced Stresses and Consolidation Settlements (CSETT)	Aug 1984
Instruction Report K-84-8	Seepage Analysis of Confined Flow Problems by the Method of Fragments (CFRAG)	Sep 1984
Instruction Report K-84-11	User's Guide for Computer Program CGFAG, Concrete General Flexure Analysis with Graphics	Sep 1984
Technical Report K-84-3	Computer-Aided Drafting and Design for Corps Structural Engineers	Oct 1984
Technical Report ATC-86-5	Decision Logic Table Formulation of ACI 318-77, Building Code Requirements for Reinforced Concrete for Automated Constraint Processing, Volumes I and II	Jun 1986
Technical Report ITL-87-2	A Case Committee Study of Finite Element Analysis of Concrete Flat Slabs	Jan 1987
Instruction Report ITL-87-1	User's Guide: Computer Program for Two-Dimensional Analysis of U-Frame Structures (CUFRAM)	Apr 1987
Instruction Report ITL-87-2	User's Guide: For Concrete Strength Investigation and Design (CASTR) in Accordance with ACI 318-83	May 1987
Technical Report ITL-87-6	Finite-Element Method Package for Solving Steady-State Seepage Problems	May 1987
Instruction Report ITL-87-3	User's Guide: A Three Dimensional Stability Analysis/Design Program (3DSAD) Module Report 1: Revision 1: General Geometry Report 2: General Loads Module Report 6: Free-Body Module	Jun 1987 Jun 1987 Sep 1989 Sep 1989

(Continued)

**WATERWAYS EXPERIMENT STATION REPORTS  
PUBLISHED UNDER THE COMPUTER-AIDED  
STRUCTURAL ENGINEERING (CASE) PROJECT**

(Continued)

	Title	Date
Instruction Report ITL-87-4	User's Guide: 2-D Frame Analysis Link Program (LINK2D)	Jun 1987
Technical Report ITL-87-4	Finite Element Studies of a Horizontally Framed Miter Gate Report 1: Initial and Refined Finite Element Models (Phases A, B, and C), Volumes I and II Report 2: Simplified Frame Model (Phase D) Report 3: Alternate Configuration Miter Gate Finite Element Studies--Open Section Report 4: Alternate Configuration Miter Gate Finite Element Studies--Closed Sections Report 5: Alternate Configuration Miter Gate Finite Element Studies--Additional Closed Sections Report 6: Elastic Buckling of Girders in Horizontally Framed Miter Gates Report 7: Application and Summary	Aug 1987
Instruction Report GL-87-1	User's Guide: UTEXAS2 Slope-Stability Package; Volume I, User's Manual	Aug 1987
Instruction Report ITL-87-5	Sliding Stability of Concrete Structures (CSLIDE)	Oct 1987
Instruction Report ITL-87-6	Criteria Specifications for and Validation of a Computer Program for the Design or Investigation of Horizontally Framed Miter Gates (CMITER)	Dec 1987
Technical Report ITL-87-8	Procedure for Static Analysis of Gravity Dams Using the Finite Element Method - Phase 1a	Jan 1988
Instruction Report ITL-88-1	User's Guide: Computer Program for Analysis of Planar Grid Structures (CGRID)	Feb 1988
Technical Report ITL-88-1	Development of Design Formulas for Ribbed Mat Foundations on Expansive Soils	Apr 1988
Technical Report ITL-88-2	User's Guide: Pile Group Graphics Display (CPGG) Post-processor to CPGA Program	Apr 1988
Instruction Report ITL-88-2	User's Guide for Design and Investigation of Horizontally Framed Miter Gates (CMITER)	Jun 1988
Instruction Report ITL-88-4	User's Guide for Revised Computer Program to Calculate Shear, Moment, and Thrust (CSMT)	Sep 1988
Instruction Report GL-87-1	User's Guide: UTEXAS2 Slope-Stability Package; Volume II, Theory	Feb 1989
Technical Report ITL-89-3	User's Guide: Pile Group Analysis (CPGA) Computer Group	Jul 1989
Technical Report ITL-89-4	CBASIN--Structural Design of Saint Anthony Falls Stilling Basins According to Corps of Engineers Criteria for Hydraulic Structures; Computer Program X0098	Aug 1989

(Continued)

**WATERWAYS EXPERIMENT STATION REPORTS  
PUBLISHED UNDER THE COMPUTER-AIDED  
STRUCTURAL ENGINEERING (CASE) PROJECT**

(Continued)

	Title	Date
Technical Report ITL-89-5	CCHAN--Structural Design of Rectangular Channels According to Corps of Engineers Criteria for Hydraulic Structures; Computer Program X0097	Aug 1989
Technical Report ITL-89-6	The Response-Spectrum Dynamic Analysis of Gravity Dams Using the Finite Element Method; Phase II	Aug 1989
Contract Report ITL-89-1	State of the Art on Expert Systems Applications in Design, Construction, and Maintenance of Structures	Sep 1989
Instruction Report ITL-90-1	User's Guide: Computer Program for Design and Analysis of Sheet Pile Walls by Classical Methods (CWALSHT)	Feb 1990
Technical Report ITL-90-3	Investigation and Design of U-Frame Structures Using Program CUFRBC Volume A: Program Criteria and Documentation Volume B: User's Guide for Basins Volume C: User's Guide for Channels	May 1990
Instruction Report ITL-90-6	User's Guide: Computer Program for Two-Dimensional Analysis of U-Frame or W-Frame Structures (CWFRAM)	Sep 1990
Instruction Report ITL-90-2	User's Guide: Pile Group--Concrete Pile Analysis Program (CPGC) Preprocessor to CPGA Program	Jun 1990
Technical Report ITL-91-3	Application of Finite Element, Grid Generation, and Scientific Visualization Techniques to 2-D and 3-D Seepage and Groundwater Modeling	Sep 1990
Instruction Report ITL-91-1	User's Guide: Computer Program for Design and Analysis of Sheet-Pile Walls by Classical Methods (CWALSHT) Including Rowe's Moment Reduction	Oct 1991
Instruction Report ITL-87-2 (Revised)	User's Guide for Concrete Strength Investigation and Design (CASTR) in Accordance with ACI 318-89	Mar 1992
Technical Report ITL-92-2	Finite Element Modeling of Welded Thick Plates for Bonneville Navigation Lock	May 1992
Technical Report ITL-92-4	Introduction to the Computation of Response Spectrum for Earthquake Loading	Jun 1992
Instruction Report ITL-92-3	Concept Design Example, Computer Aided Structural Modeling (CASM) Report 1: Scheme A Report 2: Scheme B Report 3: Scheme C	Jun 1992 Jun 1992 Jun 1992
Instruction Report ITL-92-4	User's Guide: Computer-Aided Structural Modeling (CASM) - Version 3.00	Apr 1992
Instruction Report ITL-92-5	Tutorial Guide: Computer-Aided Structural Modeling (CASM) - Version 3.00	Apr 1992

(Continued)

**WATERWAYS EXPERIMENT STATION REPORTS  
PUBLISHED UNDER THE COMPUTER-AIDED  
STRUCTURAL ENGINEERING (CASE) PROJECT**

(Concluded)

	Title	Date
Contract Report ITL-92-1	Optimization of Steel Pile Foundations Using Optimality Criteria	Jun 1992
Technical Report ITL-92-7	Refined Stress Analysis of Melvin Price Locks and Dam	Sep 1992
Contract Report ITL-92-2	Knowledge-Based Expert System for Selection and Design of Retaining Structures	Sep 1992
Contract Report ITL-92-3	Evaluation of Thermal and Incremental Construction Effects for Monoliths AL-3 and AL-5 of the Melvin Price Locks and Dam	Sep 1992
Instruction Report GL-87-1	User's Guide: UTEXAS3 Slope-Stability Package: Volume IV, User's Manual	Nov 1992
Technical Report ITL-92-12	Computer-Aided, Field-Verified Structural Evaluation Report 1: Development of Computer Modeling Techniques for Miter Lock Gates	Nov 1992